

Analytical approaches for antimalarial antibody responses to confirm historical and recent malaria transmission in malaria-endemic areas in the Philippines

Maria Lourdes M. Macalinao^{1,2,3}, Kimberly M. Fornace^{2,4}, Ralph A. Reyes¹, Alison Paolo N. Bareng¹, Tom Hall², John H. Adams⁵, Christèle Huon⁶, Chetan E. Chitnis⁶, Jennifer S. Luchavez¹, Kevin K. A. Tetteh², Katsuyuki Yui^{3,7}, Julius Clemence R. Hafalla², Fe Esperanza J. Espino¹, Chris J. Drakeley^{2*}

¹Department of Parasitology and National Reference Centre for Malaria and Other Parasites, Research Institute for Tropical Medicine, Department of Health, Muntinlupa City, Philippines; ²Faculty of Infectious Tropical Diseases, Department of Infection Biology, Faculty of Infectious and Tropical Diseases, London School of Hygiene and Tropical Medicine, London, United Kingdom; ³School of Tropical Medicine and Global Health, Nagasaki University, Nagasaki, Japan; ⁴Institute of Biodiversity, Animal Health & Comparative Medicine, University of Glasgow, Glasgow, United Kingdom; ⁵University of South Florida, Tampa, FL, 33612, USA; ⁶Malaria Parasite Biology and Vaccines Unit, Department of Parasites and Insect Vectors, Institut Pasteur, Paris, France, ⁷Shionogi Global Infectious Diseases Division, Institute of Tropical Medicine, Nagasaki University

*For correspondence: Chris.Drakeley@lshtm.ac.uk (CJD)

Abstract

Assessing the status of malaria transmission in endemic areas becomes increasingly challenging as countries approach elimination and infections become rare. Here, we evaluated the use of multiplex antibody response data to malaria-specific antigens to classify recent and historical infections of differentially exposed populations in three provinces in the Philippines. We utilized samples (n=9132) from health-facility based cross-sectional surveys in Palawan (ongoing malaria transmission), Occidental Mindoro (limited transmission), and Bataan (no transmission) and quantified antibody responses against 8 *Plasmodium falciparum* and 6 *P. vivax*-specific antigens. Different statistical and machine learning analytical methods were used to examine associations between antigen-specific antibody responses with malaria incidence, and the ability to predict recent or historical exposure. Consistent with the provinces' endemicity status, antibody levels and seroprevalence were consistently highest in Palawan and lowest in Bataan. A machine learning (ML) approach (Random Forest model) using identified responses to 4 antigens (PfGLURP R2, Etramp5.Ag1, GEXP18 and PfMSP1₁₉) gave better predictions for *P. falciparum* infection (positive by microscopy, RDT and/or PCR) or likely recent exposure in Palawan (AUC: 0.9591, CI 0.9497-0.9684) than mixture models calculating seropositivity to individual antigens. Meanwhile, employing the same ML approaches for the vivax-specific antigens did not improve predictions for recent *P. vivax* infections. Still, the antigen panel was overall able to confirm the absence of recent exposure to *P. falciparum* and *P. vivax* in both Occidental Mindoro and Bataan through single and ensemble ML approaches. Seroprevalence and seroconversion rates based on cumulative exposure markers AMA1 and MSP1₁₉ showed accurate trends of historical *P. falciparum* and *P. vivax* transmission in the 3 sites. Our study emphasizes the utility of serological markers in predicting recent and historical exposure in a sub-national elimination setting, establishes baseline antibody data for monitoring risk in malaria-endemic areas in the Philippines, and also highlights the potential use of machine learning models using multiplex antibody responses to accurately assess the malaria transmission status of countries aiming for elimination.

NOTE: This preprint reports new research that has not been certified by peer review and should not be used to guide clinical practice.

41 Introduction

42 The Philippines is aiming to eliminate malaria by 2030 following a sub-national elimination approach (**World**
43 **Health Organization, 2014**). The country had more than 70% decrease in malaria cases in the past decade,
44 with only 2 provinces reporting local cases; 19 provinces are in elimination phase, and the remaining 60
45 declared malaria-free in 2021. *Plasmodium falciparum* (Pf) contributes more than 80% to the total malaria
46 cases, *P. vivax* (Pv) is at >20%, while the other species *P. malariae*, *P. ovale* and *P. knowlesi* make up <1%
47 of the cases (**World Health Organization, 2019**). As the number of areas still reporting local cases continue
48 to decrease, assessing the malaria levels in endemic areas and differentiating areas with residual
49 transmission becomes increasingly challenging. Innovative tools that are capable of detecting both past and
50 present infections can be used to confirm the presence or absence of malaria transmission in endemic areas
51 supporting sub national specific control approaches (**Drakeley et al., 2005; malERA Refresh Consultative**
52 **Panel, 2017; World Health Organization and Global Malaria Programme, 2017**).

53 Several studies have utilized serology and malaria-specific antibody responses to estimate malaria
54 transmission intensities (**Folegatti et al., 2017; Fowkes et al., 2010**), showing that these represent a viable
55 additional metric of both historical and recent exposure (**van den Hoogen et al., 2015; Idris et al., 2017;**
56 **Kerkhof et al., 2016; Pothin et al., 2016; Ssewanyana et al., 2017; Wu et al., 2020a**). Antibody prevalence
57 alone and as age-adjusted seroconversion rates correlate with entomological and parasitological measures
58 used in estimating malaria transmission (**Corran et al., 2007; Niass et al., 2017; Staniscic et al., 2015**).
59 Many of the original studies examined single antigen platforms and antigens associated with cumulative
60 exposure to infection such as Pf apical membrane antigen-1 (PfAMA1) and the 19KDa fragment of Pf
61 merozoite protein 1 (PfMSP1₁₉). More recent advances in array and bead-based assay platforms allow for
62 simultaneous analysis of antibody responses to multiple antigens (**Fouda et al., 2006; Kerkhof et al., 2016;**
63 **Koffi et al., 2015; Ondigo et al., 2012; Perraut et al., 2014; Wu et al., 2019**). These approaches increase
64 assay throughput and allow the inclusion of multiple targets that can represent diversity in the parasite and
65 allow for variation in individual immune response. Recent multi-antigen studies have identified markers
66 associated with antibody responses describing recent and historical *P. falciparum* and *P. vivax* exposure
67 (**Helb et al., 2015; van den Hoogen et al., 2015; Longley et al., 2020; Wu et al., 2020b**). To fully realize
68 the additional information provided by examining multiple antigenic targets, these studies have employed
69 more advanced statistical approaches and algorithms such as machine learning to predict optimal
70 combinations of antibody responses for the outcome of interest.

71 The overall aim of this study was to evaluate known malaria-specific *P. falciparum* and *P. vivax* serological
72 markers for their predictive capacity to distinguish current or recent infections from historically exposed
73 individuals in order to better describe malaria endemicity in three areas of the Philippines. Specifically, we
74 sought to evaluate different approaches to determining seropositivity for estimating malaria transmission
75 intensities and exposure in areas of varying endemicity. To achieve this, we: 1) measured malaria-specific
76 antibody responses in participants recruited through health facility surveys in 3 sites in the Philippines, 2)
77 evaluated analysis methods to determine seropositivity using single and multiple antigens, and 3) analyzed
78 antibody responses and estimated transmission intensities in relation to the supposed immune status of
79 these populations. Our findings detailing the antibody responses to multiple malaria-specific antigens
80 demonstrate the utility of serology in showing the heterogeneity of malaria transmission in malaria-endemic
81 populations in the Philippine setting.

82 Methods

83 *Ethical approval*

84 This study was reviewed and approved by the Research Institute for Tropical Medicine – Institutional Review
85 Board (RITM IRB 2016-04) and LSHTM Research Ethics Committee (11597).

86 Study Sites and Samples

87 The study was conducted in 3 municipalities in 3
88 provinces in the Philippines, representing areas of
89 varying malaria endemicity 1) Rizal in the province
90 of Palawan, which is currently the most endemic
91 area in the Philippines, and reported more than
92 60% of the total cases in the country (annual
93 parasite index (API) of 5.7 per 1,000 risk
94 population) in 2018; 2) Abra de Ilog, Occidental
95 Mindoro, a municipality reporting sporadic local
96 cases at the time of the survey and with declining
97 transmission (API of 0.38 in 2018); and 3) Morong
98 in Bataan with a last reported indigenous case in
99 2011 and declared malaria-free in 2019 (Figure
100 1).

101 Participants were recruited from June 2016 to
102 June 2018 in a health facility-based rolling cross-
103 sectional survey detailed in Reyes et al (2021).
104 Briefly, all consulting patients, as well as their
105 companions, were invited to participate and
106 provide a finger-pricked blood sample for malaria
107 diagnosis through microscopy (blood smear),
108 rapid diagnostic test (RDT), and a dried blood spot
109 sample on Whatman 3MM CHR filter paper for
110 malaria diagnosis by PCR and serological
111 analysis. The DBS samples were air-dried and
112 stored in resealable bags with desiccant at 4°C
113 while in the field, and transported at ambient
114 temperatures to the laboratory facility, where it
115 was stored at 4°C and -20°C for short- and long-
116 term storage, respectively. A total of 9,132 DBS
117 samples (6572 for Palawan, 1683 for Occidental
118 Mindoro, and 877 for Bataan) were available for analysis for this study.

119 Multiplex bead-based assay of malaria-specific antibodies

120 Serological analysis was conducted using a multiplex bead-based assay as previously described (Coutts
121 et al., 2017; Helb et al., 2015; van den Hoogen et al., 2020b), with an antigen panel that included 8 *P.*
122 *falciparum*-specific and 6 *P. vivax*-specific recombinant antigens coupled to Magplex beads (Luminex Corp,
123 Austin, TX, USA). The antigens were PfAMA1 (apical membrane antigen 1), PfMSP1₁₉ (merozoite surface
124 protein), and their *P. vivax* homologues PvAMA1 and PvMSP1₁₉; PfGLURP R2 (glutamate rich protein),
125 Etramp5.Ag1 (early transcribed membrane protein 5), PfSEA1 (schizont egress antigen), GEXP18
126 (Gametocyte exported protein 18), MSP2 CH150/9 (CH150/9 allele of MSP2), MSP 2 Dd2 (Dd2 allele of
127 MSP2), PvEBP (erythrocyte binding protein), PvrBP1a (reticulocyte binding protein 1a), PvrII and PvDBPRII
128 (region II, Duffy binding protein). Antigen characteristics are shown in Table 1.

129

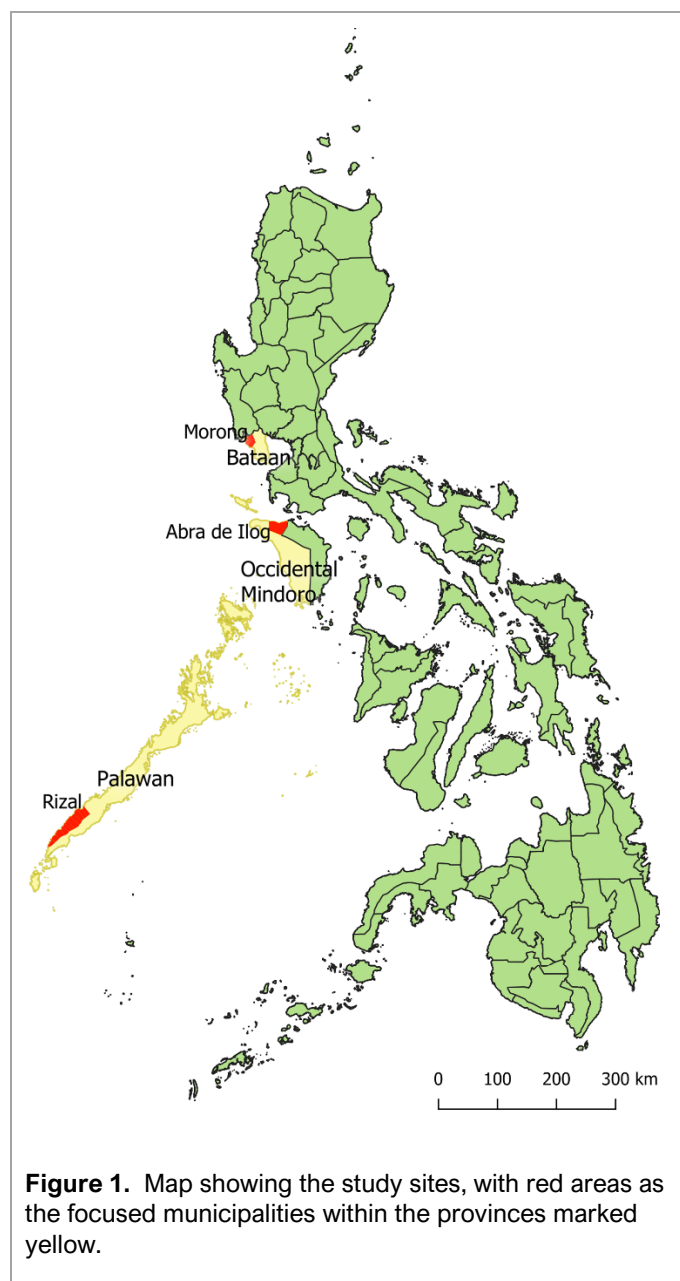


Table 1. List of antigens in the multiplex bead-based assay panel

Antigen	Description	Gene ID	Reference
<u>Pf-specific</u>			
PfAMA1	apical membrane antigen 1	PF3D7_1133400	Collins et al., 2007
PfMSP1 ₁₉	19 kDa fragment of merozoite surface protein (MSP) 1	PF3D7_0930300	Burghaus and Holder, 1994
PfGlurp R2	glutamate rich protein R2	PF3D7_1035300	Theisen et al., 1995
Etramp5.Ag1	early transcribed membrane protein 5	PF3D7_0532100	van den Hoogen et al., 2019; Spielmann et al., 2003
PfSEA1	schizont egress antigen	PF3D7_1021800	Raj et al., 2014
GEXP18	Gametocyte exported protein 18	PF3D7_0402400	Helb et al., 2015
MSP2 CH150	CH150/9 allele of MSP2	PF3D7_0206800	Polley et al., 2006
MSP2 Dd2	Dd2 allele of MSP2	PF3D7_0206800	Taylor et al., 1995
<u>Pv-specific</u>			
PvAMA1	apical membrane antigen 1	PVX_092275	Chuquiyauri et al., 2015
PvMSP1 ₁₉	merozoite surface protein	PVX_099980	França et al., 2016b
PvRII	region II, Duffy binding protein	PVX_110810	França et al., 2016a
PvDBP RII	region II, Duffy binding protein	PVX_110810	Ntumngia et al., 2012
PvEBP	erythrocyte binding protein	PVX_110835	Hester et al., 2013; Menard et al., 2013
PvRBP 1a	reticulocyte binding protein 1a	PVX_098585	França et al., 2016a

130 The assay was conducted as described in Wu et al (2019). Briefly, serum was eluted from DBS samples
 131 (~1uL from 3mm punch) with overnight incubation on a shaker and used at final dilution of 1:400.
 132 Approximately 1000 beads per antigen were added per well in 96-well flat bottom plates, and were washed
 133 using a handheld magnetic washer (Bio-Plex®) before adding 50uL of the eluted serum samples and
 134 controls, which included 2 positive controls for *P. falciparum* and *P. vivax* (pool of plasma from adults in a
 135 hyperendemic malaria setting), and 1 negative control (European malaria-naïve blood donors). After 1.5
 136 hours on a shaker, plates were washed three times with PBS-T buffer, and 50uL of 1:200 secondary antibody
 137 (Jackson Immuno 109-116-098: Goat anti-human Fcy-fragment specific IgG conjugated to R-Phycoerythrin
 138 (R-PE) was added before a further 1.5-hour incubation. After washing, samples were read using the Luminex
 139 200 machine and net median fluorescence intensity (MFI) levels to all antigens were recorded for all samples.
 140 Plate specific adjustments were performed based on the outcome of standard control curves generated
 141 from positive control pools included on each plate.

142 *Data analysis*

143 Statistical analyses were performed using R version 3.6.3 and Graphpad Prism 8. IgG antibody responses
 144 recorded as net MFI values were analyzed using different methods. Quantitative continuous antibody
 145 response data (reported as log₁₀ MFI values) were analyzed in relation to clinico-epidemiological data, and
 146 compared for different groups (*i.e.*, by age group, study site or current malaria infection) using Student's t-
 147 test or one-way ANOVA Kruskal-Wallis test with Wilcoxon test for pairwise comparisons. Correlations
 148 between the levels of antibody responses as well as age and malaria positivity were analyzed using
 149 Spearman's rank correlation.

150 *Determining seropositivity rates using single antigen responses*

151 Binary outcomes for seropositivity to each antigen were determined through the computation of cut-off
 152 values in 2 ways: by using *a.*) a 2-component finite mixture model (FMM), and *b.*) a reference naïve/ negative
 153 population (NegPop; mean MFI plus three standard deviations). The FMM was computed using the mixEM

154 function in R mixtools package, where the model identifies a negative component by modelling the log MFI
155 of the entire dataset as two normally distributed populations and identifying a threshold value from the
156 modelled negative population (mean MFI plus three standard deviations). To evaluate the accuracy of these
157 classifications, we used samples from different known exposed and unexposed populations as validation
158 data (Table 2). The validation data included a *P. falciparum* and *P. vivax*-positive group with African positive
159 controls, as well as clinical samples from a Malaysia study (**Fornace et al., 2019**) and this study. The malaria-
160 negative group consisted of European malaria-naïve samples, and Philippine malaria-negative samples from
161 individuals under 10 years of age in a 2017 cross-sectional study in Bataan (**van den Hoogen et al., 2020a**)
162 and this study. For the negative population model, the European samples were used as reference population.
163 Samples were considered seropositive for specific antigens if MFI values are higher than the antigen cutoff
164 values (mean MFI plus 3 standard deviations for each antigen). Sensitivity and specificity for identifying
165 current *P. falciparum* and *P. vivax* infection from this study and the validation dataset, as well as receiver
166 operating characteristics (ROC) curves were determined for the seropositivity results of each antigen from
167 this approach (Supplementary Tables 1 and 2).

168 *Applying machine learning techniques for multiplex analysis of antigen responses*

169 Additionally, we evaluated supervised classification approaches utilizing data from multiple antigen
170 responses. We used machine learning techniques to assess the predictive ability of all or combinations of
171 antigens for determining recent and historical malaria exposure. The 8 Pf-specific antigens were the
172 covariates evaluated for *P. falciparum* exposure, along with age. For predicting *P. vivax* exposure, the 6 Pv-
173 specific antigens were used as the covariates. Age data was not available for all the *P. vivax* training data,
174 and was therefore excluded. The training data used for these models, as detailed in Table 2, included the
175 validation dataset described, and to account for the observed age-dependent cumulative responses to the
176 antigens, the negative dataset included historical positives, which are data from survey participants aged 50
177 years and older from Malaysia and Philippines (assumed to have had some historical exposure), as well as
178 a random selection of Pf or Pv-negatives from all age groups from this current study. The historical positives
179 were used as the positive training dataset for historical exposure, and the negative population training data
180 included the same negatives from the validation dataset.

181 Super Learner (SL) optimized with AUC (Area under the ROC Curve) was used as an ensemble modelling
182 algorithm to allow for evaluating multiple models simultaneously (**Helb et al., 2015; Hubbard et al., 2013**),
183 namely Random Forest (RF), k-Nearest Neighbor (kNN), generalized boosted models (GBM), Support Vector
184 Machine (SVM), and GLM with Lasso (glmnet). Feature selection with corP, that screens for univariate
185 correlation, was also included for some component models (GBM, RF). The SL model gives a prediction
186 value that ranges from 0 to 1, and this can be used to obtain binary classification (*i.e.*, those with prediction
187 values higher than 0.5 were considered positive). A 20-fold cross-validation was performed for internal
188 validation to evaluate the performance of the fitted SL models using a portion of the training dataset withheld
189 from the model, and the whole training dataset. ROC curves were used to evaluate the outcome of predicted
190 values for the samples and were then compared to the single antigen performances. The performance of
191 each ML model, or base learner, in the SL ensemble was also assessed. For additional assessment of the
192 model performance, external validation was performed for the classification models through an independent
193 dataset from a Malaysia cross-sectional survey (**Fornace et al., 2018**), which used the same panel of *P.*
194 *falciparum* antigens (not available for *P. vivax* panel).

195 *Evaluating model performance in identifying current Pf and Pv infections in this study*

196 Antibody responses to antigens included in this study (in particular, PfGLURP R2, Etramp5.Ag1 and GEXP18)
197 have been previously shown to be predictive of recent exposure to *P. falciparum* infection (**Helb et al., 2015**;

Table 2. Training and validation data used in the classification models

Training data used	N	Validation dataset *	Negative population model	SuperLearner / Random Forest: Recent Pf exposure	SuperLearner / Random Forest: Recent Pv exposure	SuperLearner / Random Forest: Historical Pf exposure	Random Forest: Historical Pf exposure	Random Forest: Historical Pv exposure
European naive controls	179	neg	—	—	—	—	—	—
Positive controls								
African <i>P. falciparum</i> -positive	4	Pf+		+				
African <i>P. vivax</i> -positive	10	Pv+			+			
This study								
<i>P. falciparum</i> -positive subset	568	Pf+		+				
<i>P. vivax</i> microscopy-positive subset	46	Pv+			+			
Below 10 y.o. from Bataan	202	neg		—	—	—	—	—
Historical positives aged ≥50y.o. from Occidental Mindoro and Palawan	711			—		+		
PfAMA1 and PfMSP1 ₁₉ seropositive subset	512						+	
PvAMA1 and PvMSP1 ₁₉ seropositive subset	324							+
Randomly selected malaria-negatives from Palawan aged <50y.o.**	550			—	—			
Bataan study (van den Hoogen et al., 2020a)								
Below 10 y.o. from Bataan	73	neg		—	—	—	—	—
Malaysia study (Fornace et al., 2019)								
<i>P. falciparum</i> -positive subset	17	Pf+		+				
<i>P. vivax</i> -positive subset	37	Pv+			+			
Historical positives aged ≥50y.o. from Malaysia 2	1581					+		
PfAMA1 and PfMSP1 ₁₉ seropositive subset	1479			—			+	
PvAMA1 and PvMSP1 ₁₉ seropositive subset	873			—				+

* Finite mixture models (FMM) were derived from the entire ENSURE dataset (n=9132), and indicated validation dataset was used to determine receiver operating characteristics (ROC) curves for both FMM and Negative population models (seropositivity classifications from single antigens). For the supervised classification models, + means it was classified as positive for the model, and — means it is considered for negative classification. Abbreviations: Pf- *P. falciparum*, Pv- *P. vivax*, neg – malaria-negative; y.o.-years old

199 **van den Hoogen et al., 2020c**) and thus we assessed their performance using the malaria-positive samples
200 in this study (n=889). In addition to single antigens, the SL algorithm was used to generate predictive
201 outcomes based on different combinations of the covariates. The importance of the antigens in providing
202 accurate predictions were assessed by using 3 to 9 covariates at a time for the SL model (based on the
203 variable influence reported by the base learners used). The AUC values from the ROC analysis based on
204 training data and ENSURE malaria-positives data were compared among the single-antigen seropositivity
205 rates and machine learning predictions for recent exposure. For the *P. vivax* analysis, responses to all 6
206 antigens were evaluated as covariates. With Super Learner giving weights to multiple ML models assessed
207 simultaneously, we also employed for classification the individual ML models that were given the most weight
208 or importance, namely RF and GBM.

209 *Estimating seroconversion rates and historical exposure*

210 In line with previous studies, seropositivity of the cumulative exposure markers (AMA1, MSP1₁₉ for both *P.*
211 *falciparum* and *P. vivax*) were used to estimate seroconversion rates (SCR), or the rate at which seronegative
212 individuals become seropositive, and seroreversion rates (SRR), or the rate at which seropositive individuals
213 revert to being seronegative, by fitting the age-specific prevalence in each of the 3 study sites into reverse
214 catalytic models using likelihood ratio methods (**Drakeley et al., 2005; Sepúlveda et al., 2015**).
215 Seroprevalence data were fitted to models that allow for a change in SCR, and this was preferred if the
216 likelihood ratio tests result in a significant change when compared to a model assuming constant SCR. The
217 predicted time of change in transmission is then analyzed. In addition to the AMA1 and MSP1₁₉
218 seroprevalence based on FMM models, Random Forest classifications using the combined continuous data
219 of AMA1 and MSP1₁₉ net MFI values for both *P. falciparum* (Pf-RF:2-covar) and *P. vivax* (Pv-RF:2-covar)
220 were also used to generate seroprevalence curves used for the analysis. The positive training data used for
221 these RF models are subsets of the historical positives that were seropositive to both markers for each
222 species based on FMM cutoff values (Table 2). The Super Learner approach was also used to predict Pf and
223 Pv historical exposure using quantitative data from all the antigens, with analysis performed separately for
224 each species.

225 **Results**

226 *Heterogeneity of antibody responses from the 3 collection sites*

227 A total of 9132 samples from a health facility-based survey conducted from 2016 to 2018 (**Reyes et al.,**
228 **2021**) were available for serological evaluation, with the majority (>70%) from Rizal, Palawan, where the
229 monthly sampling spanned 2 years, while collection in the other sites Morong, Bataan and Abra de Ilog,
230 Occidental Mindoro spanned 1 year. Females comprised more than 60% of the total number of participants,
231 with higher proportions in Bataan and Occidental Mindoro, though individuals from all ages and gender
232 groups were represented (Table 3).

233 Malaria infections were detected only in Palawan with ~50% of infections in participants of both sexes aged
234 under 10 years old (51.8% and 48.2% males and females, respectively). Of the 889 *Plasmodium*-positive
235 samples confirmed through either microscopy, RDT and/or PCR, 58.0% had *P. falciparum*, 12.4% had *P.*
236 *vivax*, 6.7% had mixed Pf+Pv infections, 6.1% had *P. malariae*, *P. ovale* and *P. knowlesi*, while species
237 identification could not be confirmed for 16.8% of the PCR-positive samples. From the Pf and Pv malaria-
238 positive individuals (n=707, including mixed infections), 388 (54.8%) had fever before or during the visit to
239 the health facility, 62.1% of which were aged 10 years and under. Conversely, 63.1% of the asymptomatic
240 malaria infections were in individuals above 10 years old.

241 Firstly, we compared the magnitude of antibody responses to *P. falciparum* and *P. vivax* antigens from the
242 3 collection sites. Corroborating with the reported case prevalence in the area, we show that individuals

243 from Palawan consistently had the highest antibody levels to all antigens and in all age groups, followed by
 244 individuals from Occidental Mindoro then Bataan (Fig 2A, Supplementary Figure 1).

Table 3. Characteristics of study population by site

	Morong, Bataan	Abra de Ilog, Occidental Mindoro	Rizal, Palawan
Number of analyzed samples	877	1683	6572
Female, %	628 (71.6%)	1101 (65.4%)	3734 (56.8%)
Age, median (IQR) number (% in site)	26 (11-39)	28 (15-43)	13 (5-31)
0 to 5	150 (17.1%)	150 (8.9%)	1900 (28.9%)
6 to 10	63 (7.2%)	154 (9.2%)	1055 (16.1%)
11 to 19	102 (11.6%)	234 (13.9%)	957 (14.6%)
20 to 34	279 (31.8%)	508 (30.2%)	1222 (18.6%)
35 up	283 (32.3%)	637 (37.8%)	1438 (21.9%)
<i>Plasmodium</i> -positive by microscopy/RDT/PCR (% in site)*	0 (0.0%)	0 (0.0%)	889 (13.5%)
<i>P. falciparum</i> -positive (by microscopy/RDT/PCR)*	0 (0.0%)	0 (0.0%)	595 (9.1%)
<i>P. vivax</i> -positive (by microscopy/RDT/PCR)*	0 (0.0%)	0 (0.0%)	172 (2.6%)
PCR-confirmed species ID, n (% in site)			
<i>P. falciparum</i> , Pf mono-infection	0 (0.0%)	0 (0.0%)	516 (7.9%)
<i>P. vivax</i> , Pv mono-infection	0 (0.0%)	0 (0.0%)	110 (1.7%)
Pf + Pv mixed infection	0 (0.0%)	0 (0.0%)	60 (0.9%)
Other species (mono- or mixed infections)	0 (0.0%)	0 (0.0%)	55 (0.8%)
With fever or history of fever (% in site)	69 (7.9%)	172 (10.2%)	2727 (41.5%)
Symptomatic Pf and Pv infections*	0 (0.0%)	0 (0.0%)	388 (5.9%)
Asymptomatic infections (no fever, <i>Plasmodium</i> -positive)*	0 (0.0%)	0 (0.0%)	428 (6.5%)
Asymptomatic microscopy- positive Pf infections	0 (0.0%)	0 (0.0%)	132 (2.0%)
Asymptomatic microscopy- positive Pv infections	0 (0.0%)	0 (0.0%)	35 (0.5%)

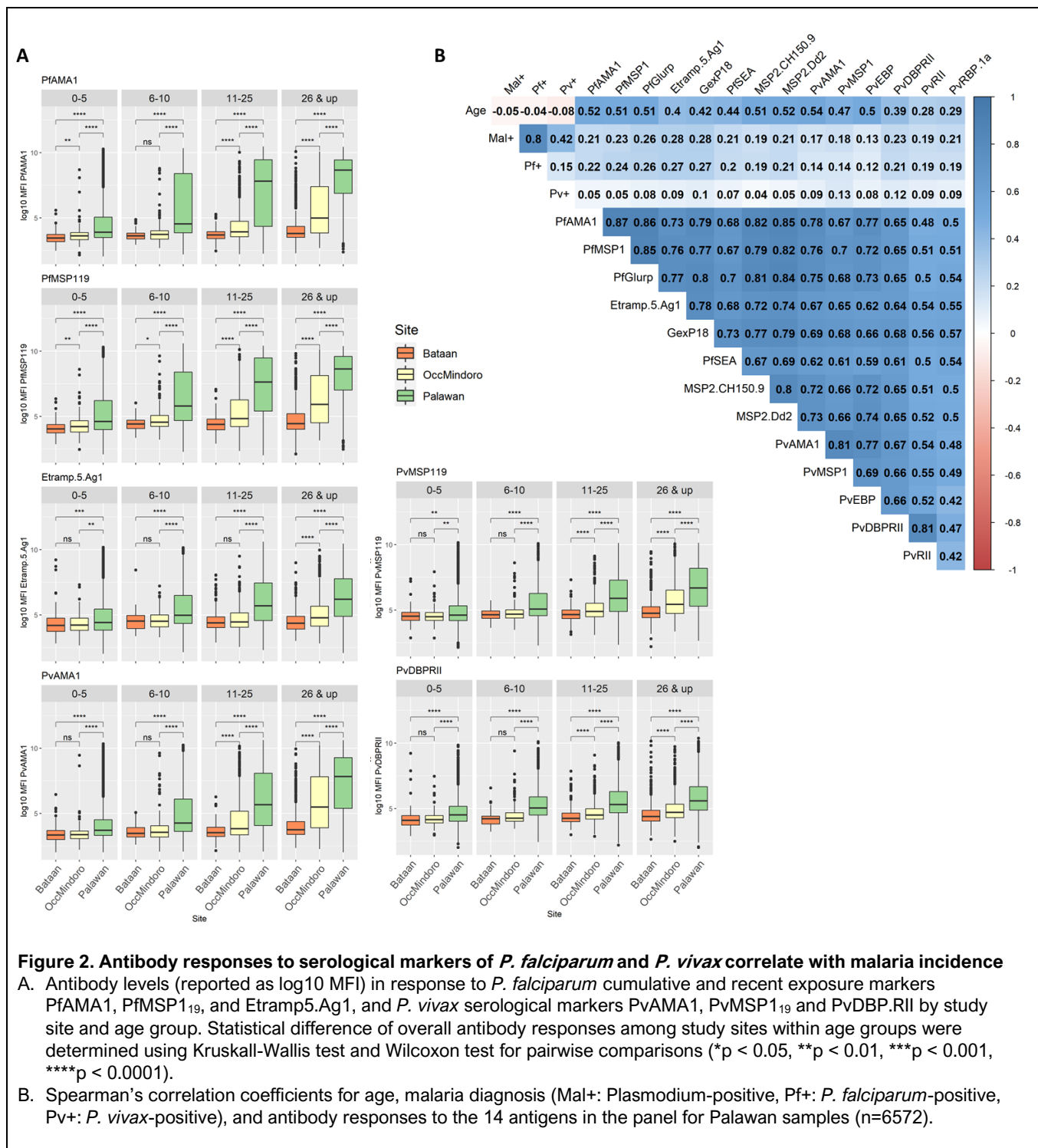
* Numbers include all *Plasmodium* infections detected by microscopy, RDT and/or PCR. Some samples did not have enough material for further species identification by PCR, for which results were based on microscopy and/or RDT diagnosis, while some (n=149) were confirmed *Plasmodium*-positive only. Pf and Pv numbers reported include mixed infections, which were specified in the PCR-confirmed species ID breakdown.

** All 5 *Plasmodium* species, including *P. malariae* (n=50), *P. ovale* (n=4) and *P. knowlesi* (n=1), were detected in Palawan, with some as co-infections with Pf and/or Pv.

245 While antibody levels increased with age in all sites, there were marked differences observed between sites.
 246 Younger age groups from Bataan and Occidental Mindoro had similar magnitude for antigens Etramp5.Ag1,
 247 PvAMA1, PvMSP1₁₉ and PvDBPRIL, which were significantly lower than in individuals from Palawan (p<0.001).
 248 The association between antibody levels and age as well as malaria positivity was then assessed for each
 249 antigen for the Palawan population, and expectedly, those associated with cumulative exposure PfAMA1,
 250 PfMSP1₁₉, PfGLURP R2, PvAMA1 and PvMSP1₁₉ were strongly correlated with age (Spearman's coefficient
 251 >0.5, p<0.0001), while those associated with recent exposure to *P. falciparum*, Etramp5.Ag1 and GEXP18,
 252 were less strongly associated (Spearman's coefficient of 0.39 and 0.42, respectively, p<0.0001), along with
 253 other *P. vivax* markers (Figure 2B). Strong positive correlations in antibody responses to all antigens were
 254 observed (Figure 2B), but the highest associations were between responses to antigens from the same
 255 species. For the *P. falciparum*-specific antigens, Etramp5.Ag1, PfGLURP R2 and GEXP18 had the stronger

256 associations with current *P. falciparum* infection (Spearman's correlation coefficient ranging from 0.26 to
 257 0.27, $p < 0.0001$), and PvMSP1₁₉ and PvDBPRII showed weak correlation (Spearman's coefficient of 0.13 and
 258 0.12, respectively, $p < 0.0001$) for current *P. vivax* infection.

259 Similarly, mean antibody levels were higher in a species-specific manner (Figure 3); Etramp5.Ag1, PfGLURP
 260 R2 and GEXP18 showed significantly higher antibody levels in those with active Pf infections ($p < 0.0001$) and
 261 PvMSP1₁₉ antibody levels were highest in *P. vivax*-positive cases ($p < 0.001$), with better resolution in younger
 262 age groups. Taken together, our results confirm the applicability of these serological markers in
 263 differentiating areas of varying malaria endemicity, and there were species-specific associations with current
 264 infection.
 265





268 *Identifying markers of recent falciparum and vivax malaria exposure and current infection*

269 Next, we applied different analytical approaches to ascertain whether the serological markers can be used
270 to predict recent or historical exposure. We first assessed the performance of responses to single antigens
271 in determining binary outcomes for seropositivity by estimating cutoff values using finite mixture models
272 (FMM) and negative population models that represented unsupervised and supervised classification models,
273 respectively (Figure 4A & 4B, Supplementary Tables 1 & 2). Seropositivity results were then compared with
274 *P. falciparum* and *P. vivax* positivity, as assessed by microscopy, RDT or PCR. The resulting seropositivity
275 cutoff values were comparable for both models, with AUC values from the validation data ranging from 0.812
276 to 0.932 for the 8 *P. falciparum* markers, and 0.534 to 0.943 for the 6 *P. vivax* markers.

277 When evaluated in classifying study samples, AUC values ranged from 0.497 to 0.756 for *P. falciparum*
278 markers and 0.513 to 0.731 for *P. vivax* markers, showing low predictive ability for some of the markers,
279 although previously reported recent exposure markers Etramp5.Ag1 and GEXP18 for *P. falciparum* and
280 PvMSP1₁₉ for *P. vivax*, had significantly higher AUC values (>0.735 , $p<0.002$) compared to the rest of the
281 markers analyzed (ranged from 0.4971 to 0.7065) (Supplementary Tables 1 & 2). Density plots of antibody
282 responses also show an overlap in samples from malaria-negative and positive individuals, contributing to
283 the lower AUCs (Supplementary Figure 2) though overall seropositivity to antigens matched with 79.2% of
284 the falciparum-positive and 60% of the vivax-positive cases in the project dataset. Proportions of samples
285 seropositive to at least 4 of the 8 Pf markers and at least 3 of 6 Pv markers were 5.02% and 5.70% for Bataan,
286 30.96% and 25.85% for Occidental Mindoro, and 53.90% and 40.03% for Palawan, respectively.
287 Seroprevalence rates for all antigens were consistently low in Bataan in all age groups as shown in Figures
288 4A & 4B, with recent exposure markers (hollow circles) estimating lower rates, consistent with their lower
289 correlation with age and lower likelihood of exposure to infection in this setting.

290 To analyze the multi-antigen continuous antibody data, we used supervised machine learning methods for
291 antibody responses to antigens for both species. The Super Learner (SL) ensemble machine learning
292 algorithm was used to simultaneously evaluate machine learning models, which included Random Forest
293 (RF), k-Nearest Neighbor (kNN), generalized boosted models (GBM), Support Vector Machine (SVM), and
294 GLM with Lasso (glmnet), in predicting recent and historical malaria exposure through the resulting weights
295 applied to each learner after cross-validation. Different combinations of covariates were assessed for their
296 relative importance for the model using the ROC curves of the cross-validated predictions (Figure 4C & 4D;
297 Supplementary Tables 1 & 2). A 9-covariate model (SL: 9-covar) was evaluated for the Pf panel, which had
298 the antibody responses to 8 antigens and age as covariates. This model had the highest AUC among all SL
299 models, with a value of 0.9898 (95% CI 0.9874-0.9921) and 0.9197 (95% CI 0.9093-0.9302) for the binary
300 classification predictions for the training data and test data, respectively. It was able to correctly identify
301 71.1% of the *P. falciparum*-positive individuals from this study (Supplementary Table 1). Removing the age
302 as covariate (SL:8-covar model) decreased the prediction capacity of the model for the test data, with 53.3%
303 of the *P. falciparum* infections identified. For predicting *P. vivax* recent exposure, *i.e.*, confirmed Pv infections,
304 the 6 Pv antigens were used as covariates for the SL model (SL:6-covar) and had a resulting AUC of 0.8857
305 (95% CI 0.8429-0.9284) and 0.6332 (0.5979-0.6686) for validation data and test data, respectively
306 (Supplementary Table 2).

307 Super Learner assigns weights to each machine learning model included in the ensemble algorithm after
308 cross-validation, and for both Pf and Pv exposure predictions, generalized boosted models with or without
309 feature selection (GBM and GBM_corP) were given the highest weights, followed by 3 included variations of
310 the RF model (RF, RF-ranger and RF-ranger_corP) (Supplementary Figure 3A & 3B). However, upon using
311 20-fold nested cross-validation and closer inspection of the classification accuracy of the individual learners,
312 the Random Forest (RF) models were found to have the highest AUCs for predicting *P. falciparum* recent
313 infections in both the validation data (not shown) and test data (Supplementary Figure 3C), while component

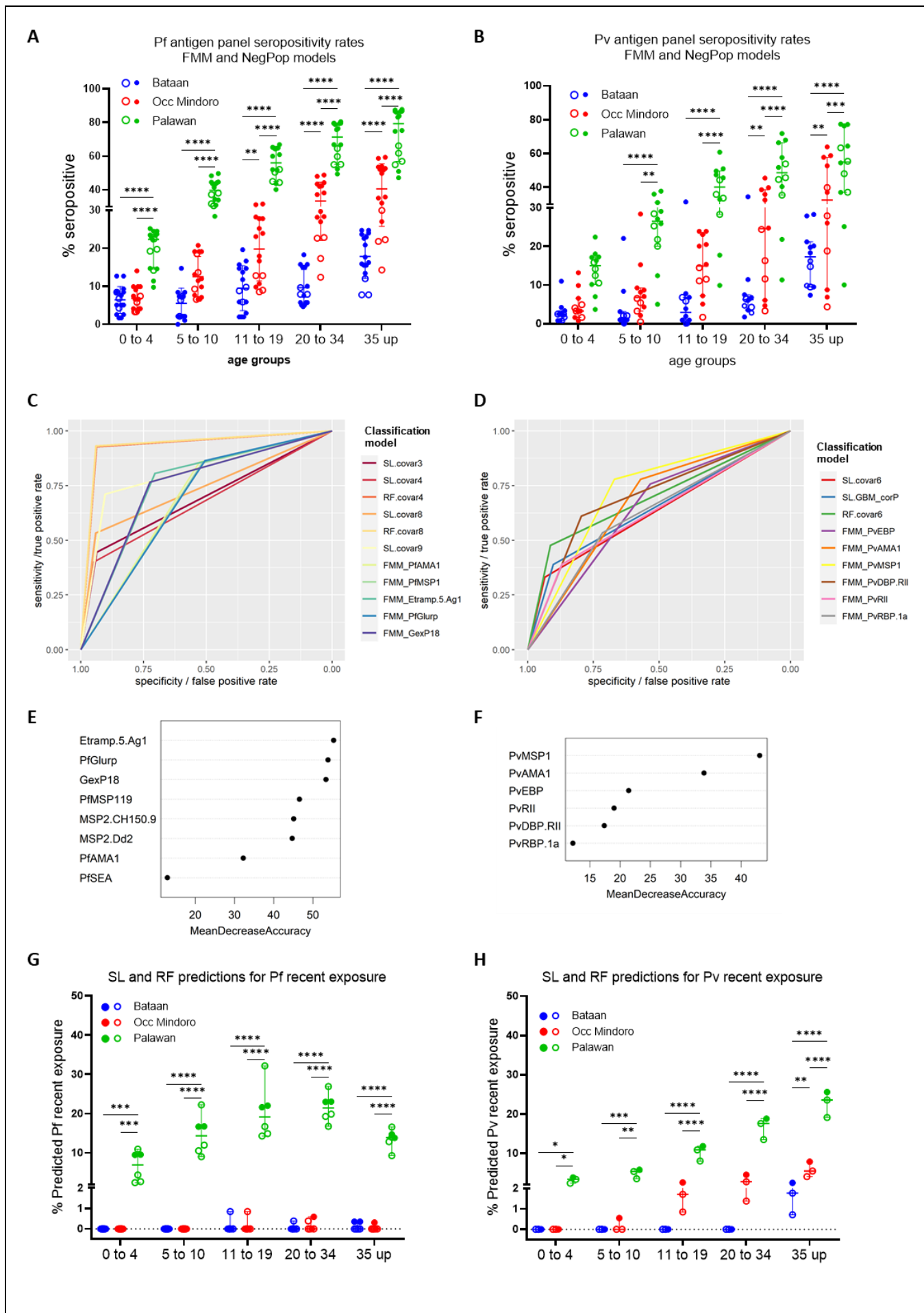


Figure 4. Analysis of serological markers through machine learning methods improves classifications for recent *P. falciparum* and *P. vivax* exposure or current infection

A-B. Seropositivity rates of sample population by site and age group based on cutoff values from finite mixture models (FMM) and negative population model (NegPop) for Pf and Pv antigens (detailed in **Supplementary Tables 1 and 2**). Hollow dots represent the FMM and Negpop seropositivity rates for the two reported recent exposure markers Etramp5.Ag1 and GEXP18 for Pf (A), and PvMSP1₁₉ and PvDBP.RII for Pv (B) panel. Lines with error bars represent median with 95% CI.

C-D. Receiver operating characteristic (ROC) curves for the antibody responses to single antigens for individual antigens, and for the SL models (shown in both as binary outcomes of seropositivity / prediction values).

E-F. Variable importance of the 8 Pf-specific (E) and 6 Pv-specific (F) antigens based on the Random Forest model.

G. Predicted rates of recent Pf exposure based on analysis of the continuous antibody responses of the 8-antigen panel using Super Learner. Each hollow dot represents differences in the number of covariates used for the model (3, 4, 8, 9), as well as 2 showing rates from prediction values of the Random Forests (RF) component model (RF.covar4 and RF.covar8 in solid dots).

H. Predicted rates of recent Pv exposure based on analysis of the continuous antibody responses of the 6-antigen panel using Super Learner. Dots represent the positivity rates from the prediction values of the SL model, and the individual predictions from the 2 most weighted base learners in the resulting model – RF and GBM. RF predictions (RF.covar6) are shown as solid dots.

(SL: Super Learner, RF: random Forest, covar#: number of covariates included in the model, FMM: finite mixture models; *p < 0.05, **p < 0.01, ***p < 0.001, ****p < 0.0001 with significance assessed by one-way ANOVA followed by Tukey's multiple comparison)

314 models for classifying vivax malaria infections had similar AUCs, ranging from 0.701 to 0.8 for test data
315 (Supplementary Figure 3D).

316 The Super Learner ensemble model did not show any increase in classification accuracy compared to RF,
317 which suggests that RF is the best performing model in distinguishing current or recent falciparum malaria
318 infections. Still, both SL and SL-RF (RF prediction within the SL ensemble) predictions from the Pf panel had
319 highly improved AUCs compared to single antigen classifications based on finite mixture models (Figure 4C),
320 while model predictions for the Pv panel had comparable AUCs, and machine learning models did not
321 improve the AUC predictions (Figure 4D). Variable importance in the RF model shows that responses to
322 Etramp5.Ag1, PfGLURP R2, GEXP18 and PfMSP1₁₉ had the highest influence in the predictions for *P.*
323 *falciparum* positivity (Figure 4E), while PvMSP1₁₉ and PvAMA1 were the most predictive *P. vivax* antigens
324 (Figure 4F). Using the top 3 antigens (SL:3-covar - PfGLURP R2, Etramp5.Ag1, GEXP18) and top 4 (SL:4-
325 covar, which included PfMSP1₁₉) as covariates resulted in further lowered AUC values with 0.8790 and
326 0.8967, respectively, and identified >50% of the *P. falciparum* cases (Supplementary Table 1).

327 Performing Random Forest models outside SL (using Random Forest package) had the same predictions as
328 SL-RF, and using the 4 covariates Etramp5.Ag1, PfGLURP R2, GEXP18 and PfMSP1₁₉ (RF.covar4) gave an
329 AUC of 0.9983 for the training data and 0.9591 for the test data – the highest for all Pf models tested (Figure
330 3C; Supplementary Table 1). The RF.covar4 model was able to accurately identify 92.8% of the *P. falciparum*
331 infections in our data, and had a comparable AUC with the RF 8-covariate model (RF.covar8), showing that
332 analysis using the 4 antigens is sufficient for predicting recent *P. falciparum* infection or exposure (Figure
333 3C; Supplementary Table 1). Meanwhile, predictions of *P. vivax* recent exposure were also not different for
334 the SL, RF and GBM models (Figure 4D; Supplementary Table 2).

335 The predictive performance of the resulting SL models (SL:3-covar, SL:4-covar, SL:8-covar, SL:9-covar for
336 Pf exposure predictions, and SL:6-covar for Pv exposure predictions) were then compared with RF (both
337 species) and GBM (for Pv) predictions (RF.covar4 and RF.covar8 for Pf; RF.covar6 and GBM.covar6 for Pv)
338 (Figure 4G & 4H), and the rates of predicted current *P. falciparum* infection based on SL and RF models all
339 consistently gave 0-0.2% prediction for Occidental Mindoro and Bataan, where no *P. falciparum* malaria
340 cases were reported in recent years, suggesting that these models can accurately predict the absence of
341 recent falciparum malaria exposure and infection (Figure 4G). Analysis of antibody responses to *P. vivax*

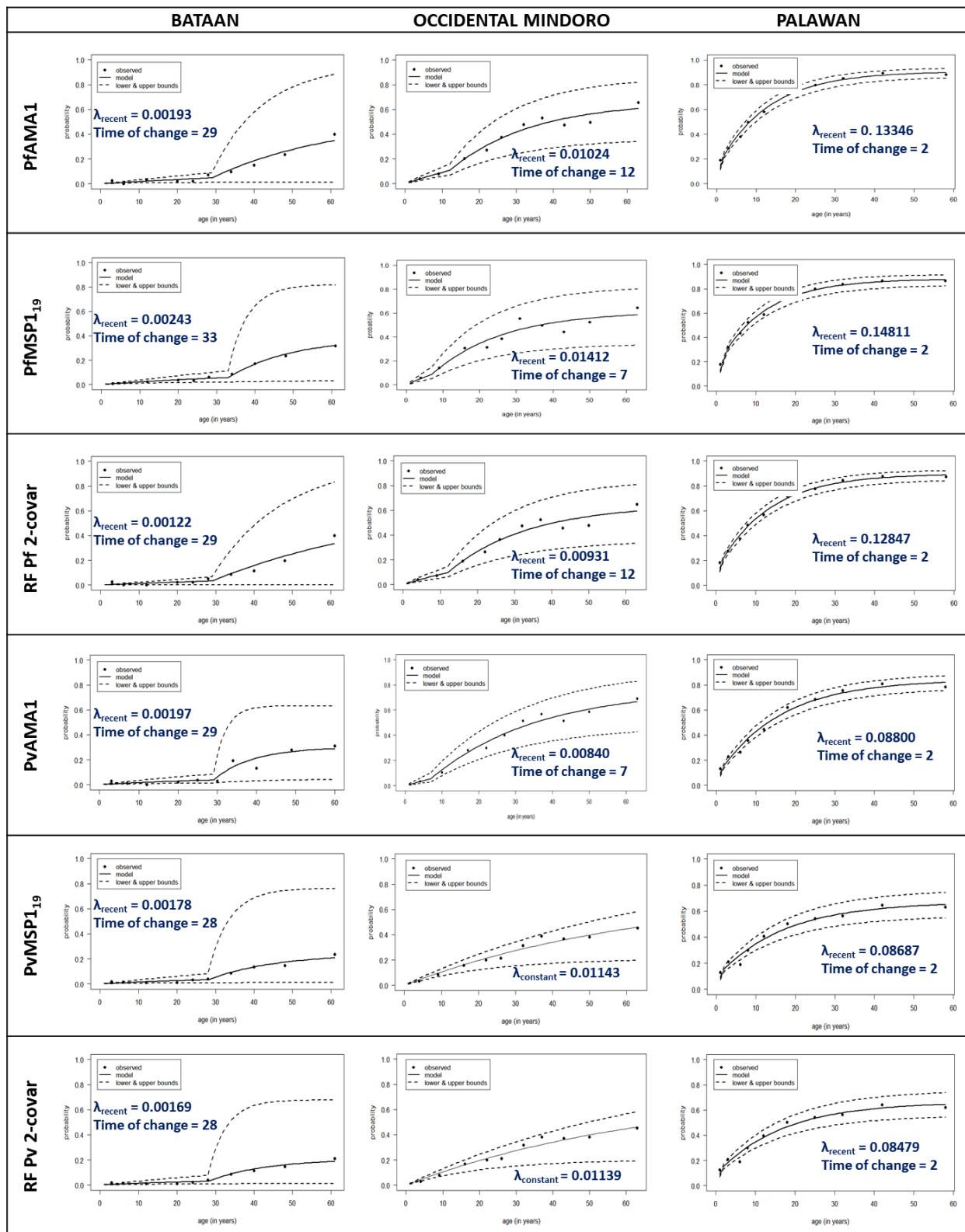


Figure 5. Seroconversion curves based on reverse catalytic models using AMA1 and MSP1₁₉ antibody responses provide accurate estimates of historical exposure. Age-specific seroprevalence was based on finite mixture models and Random Forest models (using both antigens: RF 2-covar models) for each species. Solid lines represent the fit of the reversible catalytic models, dashed lines represent 95% confidence intervals, and dots represent the observed proportions of seropositives per age divided into 10% centiles. For models assuming a change point in transmission, only the recent seroconversion rates and change point estimates (in years) are shown, while the historical seroconversion rates and seroreversion rates are detailed in Table 4.

342 antigens also had <1% prediction rate for Bataan and <5% for Occidental Mindoro, also indicative of the
343 absence of recent *P. vivax* infections in these sites (Figure 4H; Supplementary Table 2).

344 To further evaluate the performance of the RF 4-covariate model for predicting *P. falciparum* recent
345 exposure, external validation was performed using an available test dataset that included samples from a
346 cross-sectional survey in Malaysia (n=8163; **Fornace et al., 2018**), PCR-validated malaria cases (Pf=47, non-
347 Pf=423), and malaria-naïve or malaria-negative samples (n=511). The model prediction resulted in an AUC
348 of 0.93 (CI 0.8817-0.9782), and was able to predict 0.47% prevalence of infection for the cross-sectional
349 survey, correctly identifying 41 of 47 (87.2%) of the *P. falciparum* PCR-confirmed cases seen in the survey.
350 The observation that this relatively simple model was able to provide accurate predictions for both the
351 Philippine and Malaysian datasets suggests potential as a robust indicator for recent exposure and current
352 infections, in areas with varying levels of transmission.

353 *Estimating P. falciparum and P. vivax historical exposure*

354 AMA1 and MSP1₁₉ responses for *P. falciparum* and *P. vivax* have been widely used to assess historical

Table 4. Seroconversion and seroreversion rates from reverse catalytic models in each study site

		Bataan	Occidental Mindoro	Palawan
PfAMA1	SCR _{historical}	0.02102 (0.00599 - 0.07375)	0.03306 (0.02150 - 0.05082)	0.06953 (0.06251 - 0.07736)
	SCR _{recent}	0.00193 (0.00112 - 0.00332)	0.01024 (0.00707 - 0.01483)	0.13346 (0.11802 - 0.15092)
	SRR	0.010002 (0.0010 - 0.10353)	0.01239 (0.00575 - 0.02673)	0.00841 (0.00626 - 0.01129)
	Time of change in transmission (yrs)	29	12	2
PfMSP1 ₁₉	SCR _{historical}	0.04042 (0.00836 - 0.19516)	0.03399 (0.02221 - 0.05204)	0.07521 (0.06658 - 0.08495)
	SCR _{recent}	0.00243 (0.00148 - 0.00396)	0.01412 (0.00842 - 0.02367)	0.14811 (0.13109 - 0.16734)
	SRR	0.01959 (0.00564 - 0.06796)	0.01779 (0.00926 - 0.03416)	0.01221 (0.00946 - 0.01575)
	Time of change in transmission (yrs)	33	7	2
RF with PfAMA1 and PfMSP1 ₁₉	SCR _{historical}	0.01513 (0.00426 - 0.05370)	0.03338 (0.02172 - 0.05130)	0.06836 (0.06133 - 0.07619)
	SCR _{recent}	0.00122 (0.00064 - 0.00234)	0.00931 (0.00630 - 0.01377)	0.12847 (0.11333 - 0.14564)
	SRR	0.00463 (0.00002 - 0.91264)	0.01327 (0.00639 - 0.02755)	0.00901 (0.00674 - 0.01204)
	Time of change in transmission (yrs)	29	12	2
PvAMA1	SCR _{historical}	0.07078 (0.01619 - 0.30943)	0.02760 (0.02094 - 0.03638)	0.05210 (0.04652 - 0.05834)
	SCR _{recent}	0.00197 (0.00102 - 0.00377)	0.00840 (0.00451 - 0.01564)	0.08800 (0.07591 - 0.10202)
	SRR	0.03138 (0.01524 - 0.06460)	0.00715 (0.00269 - 0.01898)	0.01074 (0.00801 - 0.01441)
	Time of change in transmission (yrs)	29	7	2
PvMSP1 ₁₉	SCR _{historical}	0.02858 (0.00465 - 0.17570)	0.01143 (0.00921 - 0.01419)	0.03760 (0.03172 - 0.04458)
	SCR _{recent}	0.00178 (0.00092 - 0.00347)		0.08687 (0.07507 - 0.10052)
	SRR	0.02941 (0.00862 - 0.10026)	0.00404 (0.00047 - 0.03486)	0.02146 (0.01599 - 0.02880)
	Time of change in transmission (yrs)	28	-	2
RF with PvAMA1 and PvMSP1 ₁₉	SCR _{historical}	0.03387 (0.00559 - 0.20521)	0.01139 (0.00919 - 0.01414)	0.04023 (0.03472 - 0.04661)
	SCR _{recent}	0.00169 (0.00084 - 0.00340)		0.08479 (0.07313 - 0.09833)
	SRR	0.03498 (0.01265 - 0.09673)	0.00388 (0.00042 - 0.03598)	0.02227 (0.01674 - 0.02963)
	Time of change in transmission (yrs)	28	-	2

Seroconversion rates (SCR) and seroreversion rates (SRR) are presented for *P. falciparum* and *P. vivax* based on reverse catalytic models using age-specific seroprevalence from finite mixture models with AMA1 and MSP1₁₉ and Random Forest (RF) 2-covariate models. If the best reverse catalytic model to fit the age-adjusted seropositivity data was one with no change point in transmission, only 1 SCR is indicated, while if the best fit is one with a change point, the SCR before the change point is indicated as SCR_{historical} and the SCR after the change point is indicated as SCR_{recent}. The estimated change point in transmission (in years) is also indicated.

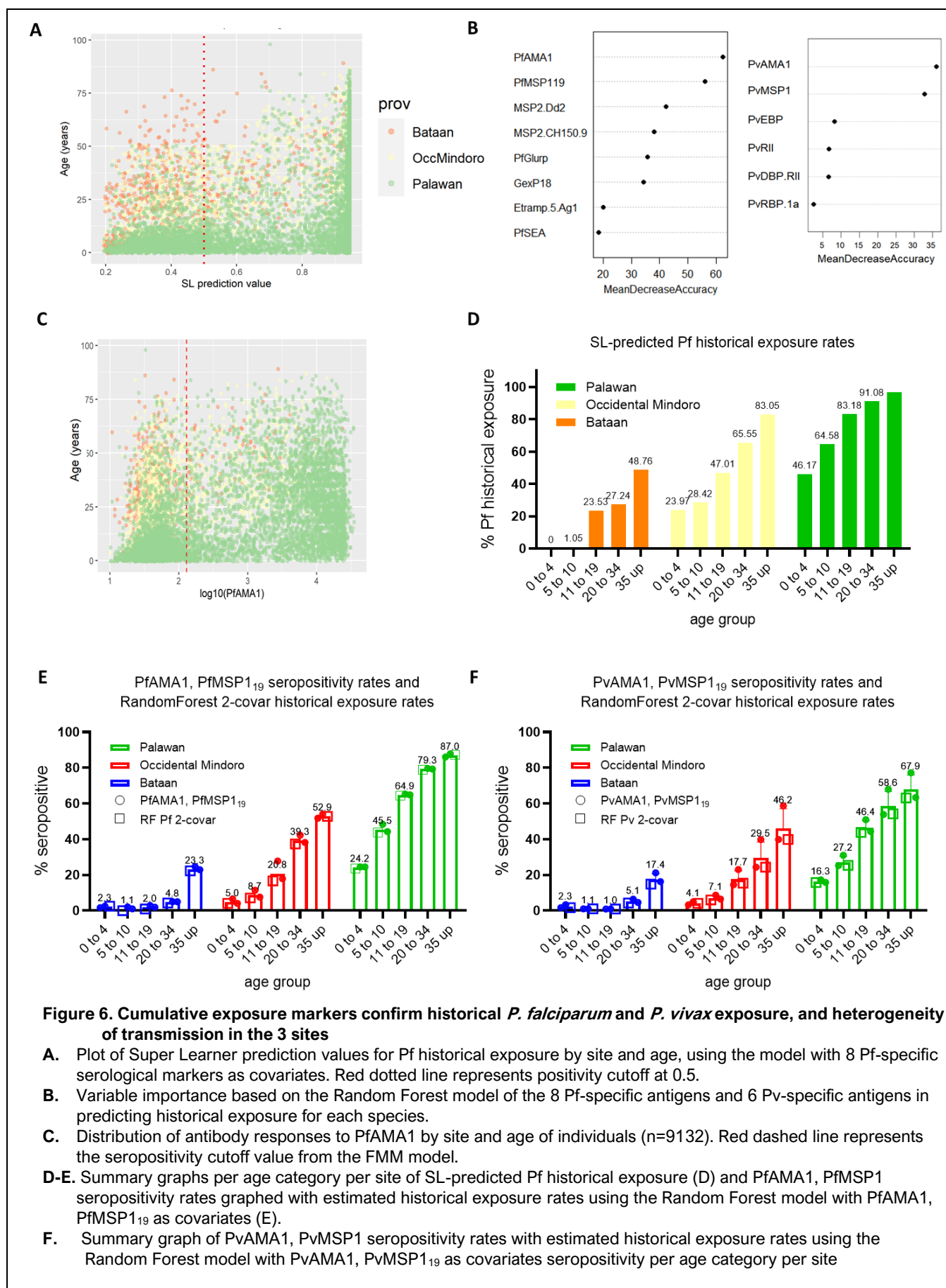


Figure 6. Cumulative exposure markers confirm historical *P. falciparum* and *P. vivax* exposure, and heterogeneity of transmission in the 3 sites

- A.** Plot of Super Learner prediction values for Pf historical exposure by site and age, using the model with 8 Pf-specific serological markers as covariates. Red dotted line represents positivity cutoff at 0.5.
- B.** Variable importance based on the Random Forest model of the 8 Pf-specific antigens and 6 Pv-specific antigens in predicting historical exposure for each species.
- C.** Distribution of antibody responses to PfAMA1 by site and age of individuals (n=9132). Red dashed line represents the seropositivity cutoff value from the FMM model.
- D-E.** Summary graphs per age category per site of SL-predicted Pf historical exposure (D) and PfAMA1, PfMSP1 seropositivity rates graphed with estimated historical exposure rates using the Random Forest model with PfAMA1, PfMSP1₁₉ as covariates (E).
- F.** Summary graph of PvAMA1, PvMSP1 seropositivity rates with estimated historical exposure rates using the Random Forest model with PvAMA1, PvMSP1₁₉ as covariates seropositivity per age category per site

356 exposure by estimating seroconversion and seroreversion rates. Using reverse catalytic models and
357 maximum likelihood tests on the age-specific seroprevalence based on the FMM model seropositivity rates
358 for PfAMA1, PfMSP1₁₉, PvAMA1 and PvMSP1₁₉, we estimated the time of interruption of transmission in our
359 study area (Figure 5, Table 4).

360 The Random Forest algorithm was also employed to generate models that make use of both cumulative
361 exposure antigens (2-covariate models for the 2 species: Pf-RF:2-covar and Pv-RF:2-covar), and the
362 predicted binary outcomes were also used in the reverse catalytic models. Most of the seroconversion
363 curves were best fit with a model assuming a change in transmission based on log likelihood tests ($p <$
364 0.001), except for PvMSP1₁₉ ($p = 0.507$) and the RF-Pv model ($p = 0.285$) with PvAMA1 and PvMSP1₁₉ as
365 covariates (Table 4).

366 Based on these models, the time of change in transmission in Bataan was estimated at 29-33 years for *P.*
367 *falciparum* and 28-29 years for *P. vivax*. Occidental Mindoro had varied estimates of the change point (7 and
368 12 years), while PvMSP1₁₉ and consequently the RF Pv 2-covar model did not better fit in the model
369 assuming a change in transmission. For these 2 provinces, the seroconversion rates were decreased after
370 the change point, suggesting a decrease in transmission, while for Palawan, an increase of the
371 seroconversion rates was observed in all models after the 2-year change point, suggesting that there was
372 an increase in transmission in this study site.

373 We further explored whether the use of the SL model can provide improved estimates of historical exposure.
374 The 8 Pf antigens and 6 Pv antigens were separately used as covariates, and the binary classification derived
375 from the SL prediction values for each site by age group were then compared with the single antigen
376 seropositivity rates and RF 2-covariate models' estimated exposure rates (Figure 6A & 6C, summarized in
377 Figure 6D & 6E, respectively). The contribution of each covariate based on the RF model (Figure 6B), as
378 expected, showed that the antigens associated with long-lived antibody responses – AMA1 and MSP1₁₉ –
379 had the highest influence in the prediction for both *P. falciparum* and *P. vivax* historical exposure. However,
380 comparing the SL-predicted rates with seropositivity rates of the top Pf antigen PfAMA1 (Figure 6A & 6B)
381 show that SL overestimated historical exposure, with higher-than-expected positivity rates observed in
382 younger age groups from Bataan and Occidental Mindoro where transmission is reportedly absent (Figure
383 6E). The seropositivity rates based on the 2-covariate RF models with AMA1 and MSP1₁₉ seem to provide
384 better estimates of historical exposure to both *P. falciparum* and *P. vivax* based on known malaria prevalence
385 of the sites than the SL models that included all antigens (Figure 6E & 6F).

386 Discussion

387 In this study we assessed the utility of multiple antigen specific antibody responses and different statistical
388 methods to estimate both current malaria infection and historical transmission in areas of different
389 endemicity in the Philippines. Using a multiplex bead-based assay with a panel of 8 *P. falciparum*-specific
390 and 6 *P. vivax*-specific recombinant antigens, we showed that whilst antibody levels to most antigens
391 described broad differences in transmission, Random Forest predictions with 4 *P. falciparum*-specific
392 antigens (Etramp5.Ag1, PfGLURP R2, GEXP18 and PfMSP1₁₉) accurately identified >90% of *P. falciparum*
393 infections in the data. Rates of predicted infection with these models were also highly consistent with ongoing
394 levels of transmission described by routine data. Similar observations were made for *P. vivax* with 2 antigens
395 (PvMSP1₁₉ and PvAMA1) but with lower precision. Moreover, reconstruction of historical transmission
396 patterns was improved by combining seropositivity to two antigens (MSP1₁₉ and AMA1 for both *P. falciparum*
397 and *P. vivax*) assessed using finite mixture models, and further improved using the Random Forest model
398 on continuous data from these antigens combined. These findings highlight the potential for advanced

399 analysis of multiplex serological data to provide additional accurate data on incidence levels that could be
400 used by control programs at small spatial scales.

401 The use of multiple antigens to assess exposure to malaria infection circumvents some issues related to
402 genetic diversity in the parasite and variation in the human immune response to different antigenic targets.
403 The approach also allows application of more advanced statistical analysis to examine optimal combinations
404 of antibody responses in predicting specific outcomes. Here, in addition to the well-studied antigens AMA1
405 and MSP1₁₉, we screened other antigenic markers that have been reported to accurately predict recent
406 exposure in studies in Africa and the Caribbean (Helb et al., 2015; van den Hoogen et al., 2020c; Wu et
407 al., 2020a). We then employed a machine learning approach for predicting classification outcomes of
408 disease exposure which has been used previously to analyze antibody response data (Helb et al., 2015;
409 Longley et al., 2020; Rosado et al., 2020). We showed that the machine learning models were able to both
410 confirm the absence of current infection in Occidental Mindoro and Bataan, and, using the Random Forest
411 predictions from a 4-covariate model including PfGLURP R2, Etramp5.Ag1, GEXP18 and PfMSP1₁₉,
412 accurately identify >92% of the *Plasmodium*-positive study samples from this study, whether detected
413 through microscopy, RDT and/or PCR. The relative simplicity of this model and lack of requirement for basic
414 epidemiological variables such as age is a benefit in assessing current infection and recent exposure,
415 including stable transmission settings (i.e., like in Palawan with an API of >5 for the whole province, and >30
416 for the study site Rizal). We expected that the Super Learner model would improve the predictions with its
417 ensemble approach; however, for predicting *P. falciparum* current infections in particular, RF-based models
418 had the better AUC for both training and test data. This was not the case for the *P. vivax* current infection
419 predictions, which showed similar AUCs (<0.7) for the final SL model and its component models. RF variable
420 importance showed that PvMSP1₁₉ was the most predictive among the 6 antigens in our panel, which is
421 consistent with the recent study by Longley et al (2020), likewise utilizing a RF prediction algorithm that
422 identified PvMSP1₁₉ as one of the 8 most predictive *P. vivax* recent exposure markers. It is likely that the low
423 AUC and predictive ability we observed is a limitation of the panel of antigens available to us at the time of
424 the study rather than the analytical approach itself. Notwithstanding, the SL approach was able to provide
425 the means for evaluating multiple supervised machine learning models simultaneously, and, for the purpose
426 of accurately distinguishing recent exposure from historical exposure with high sensitivity, the RF model
427 seems to be the most predictive. The satisfactory results from the external validation using the cross-
428 sectional survey data from Malaysia also suggests broader utility not least in neighboring Southeast Asian
429 countries with similar historical transmission patterns.

430 In stratification of malaria transmission, a key component is determining its absence. In many countries
431 including the Philippines, malaria-endemic provinces apply for malaria-free status when indigenous or local
432 cases have not been reported for a set number of years, typically 3 or more. More rapid, subnational
433 demonstration of the absence of exposure could aid in this process. Cumulative exposure markers are used
434 in various studies to estimate malaria transmission intensities, wherein age-specific seroprevalence can be
435 used to confirm the level of historical exposure of endemic areas. Malaria-specific serological assays can
436 then be utilized for determining the absence of transmission by evaluating antibody responses of populations.
437 In assessing the individual performances of recent exposure markers, it can be observed that younger age
438 groups in Bataan reported <10% seropositivity, although this province has not reported indigenous cases
439 since 2011, and this may be attributed to background seropositivity. Moreover, the lower seropositivity rates
440 observed in younger age groups in Palawan may be attributed to children who have not yet developed
441 adequate IgG responses for detection in a serological assay. Nevertheless, our results provide an alternative
442 approach using a multiplex analysis of 4 predictive *P. falciparum* serological markers that was able to
443 improve the computation of binary outcomes for accurately predicting current or recent falciparum malaria
444 infections.

445 Strong correlations among the *P. falciparum* and *P. vivax* antigens in the panel were observed, consistent
446 with previous observations (**Chotirat et al., 2021; Rogier et al., 2021**) and suggesting the combined risk of
447 *P. falciparum* and *P. vivax* infection in Rizal, Palawan. Nonetheless, our results also indicate that the *P.*
448 *falciparum*-positive and *P. vivax*-positive samples had species-specific increase and significantly different
449 patterns in its antibody responses to the *P. falciparum* and *P. vivax*-specific antigens. The simultaneous
450 cumulative increase in species-specific antibodies has been explored for its possible role in the development
451 of cross-protective immunity (**Gnidehou et al., 2019; Mitran and Yanow, 2020; Muh et al., 2020**), and can
452 be an area for further investigation, as this could potentially explain the observed asymptomatic PCR-only
453 cases (including mixed infections) in Rizal, Palawan (**Reyes et al., 2021**).

454 This study had a number of limitations. Since the study analyzed samples from a health facility-based survey,
455 whether or not it accurately represents the populations needs to be assessed. Due to the nature of the
456 survey we were only able to sample health-seeking individuals, though this was partially addressed by also
457 recruiting companions of patients who visited the health facilities (**Reyes et al., 2021**). For predicting recent
458 infections, we had not asked survey participants if they recently had malaria, or if they had past malaria
459 episodes for that matter (self-reported malaria history), such that we have only attempted to predict current
460 infections. Still, external validation of our prediction algorithm for *P. falciparum* infection confirms its
461 promising performance in accurately predicting malaria infections.

462 There are also no accessible detailed records of the malaria history of individual visitors in the health facilities,
463 such that the results for the predicted historical exposure cannot be validated. Nonetheless, we are able to
464 show that consistent with previous studies (**Biggs et al., 2017; Idris et al., 2017; Perraut et al., 2014;**
465 **Rosas-Aguirre et al., 2015; Wu et al., 2020b**), seropositivity rates from cumulative exposure markers AMA1
466 and MSP1₁₉ for *P. falciparum* and *P. vivax* seemed to agree with the known malaria situation of our study
467 sites. The “historical positives” used as training data for predicting historical exposure were the adult
468 population (aged 50 years old and above) in malaria-endemic areas, wherein we assumed that all these
469 individuals were exposed at some point, and that their antibody profiles would reflect historical exposure.
470 The high variations in the dataset would have greatly affected these predictions. Since the reference
471 population data available for predicting historical exposure using supervised classification approaches was
472 not suitable, using the unsupervised approach of determining AMA1 and MSP1₁₉ seropositivity rates based
473 on FMM may then suffice. Based on the known malaria situation in the collection sites, results from the SL
474 model, RF 2-covar model and individual seropositivity rates of AMA1 and MSP1₁₉ may be able to provide a
475 reliable estimate of malaria exposure in the area. The seroconversion rates also reflect the transmission
476 status of our sites, with Bataan having the lowest, followed by Occidental Mindoro, and highest for Palawan.
477 Our results are able to confirm the absence of *P. falciparum* and *P. vivax* transmission in malaria-free Bataan
478 for the age groups 10 and below, providing evidence for its malaria elimination status. Moreover, the change
479 point in transmission for Bataan is estimated higher but still consistent with the results of a serological survey
480 conducted in the same area a year prior, which estimated the change point at 22 years (**van den Hoogen**
481 **et al., 2020a**), and coincided with the decline in cases in the municipality. For Occidental Mindoro, the
482 interruption in transmission from 7-12 years ago may be explained by the extensive malaria control activities
483 implemented in the area, as the province has been part of the priority provinces of the Global Fund for
484 Malaria since the 2000s. Our seroconversion curve results also suggest an increase in malaria transmission
485 in Rizal, Palawan during the time of our survey (2016 to 2018), and upon checking the numbers of the
486 reported malaria cases, there was indeed a steady rise of the API in this municipality from 25.43 in 2014,
487 33.97 in 2015, to 46.09 in 2016 and 56.78 in 2018.

488 The longevity of IgG antibody responses to malaria-specific antigens has the potential to also provide
489 information on the development of naturally acquired immunity in populations (**King et al., 2015**) – although
490 if and how assay responses translate to immune protection is not well understood (**Crompton et al., 2010**;

491 **Proietti et al., 2019; Stanisic et al., 2015**). From the 3 sites in the study, we were able to detect *Plasmodium*
492 infections only in Rizal, Palawan. Asymptomatic infections comprised 265 (44.5%) of the malaria cases
493 detected, and were observed in all age groups, which suggests the development of clinical immunity in this
494 endemic population with relatively stable transmission. Our results showed that >80% of the PfAMA1
495 seropositives in Bataan had lived there for >10 years, and had net MFI levels that were comparable with
496 adults in Occidental Mindoro and Palawan (data not shown), suggesting that what we observed could be
497 long-lived antibody responses to *P. falciparum* and *P. vivax* malaria in the population. Still, the lower
498 seropositivity rates in Bataan and Occidental Mindoro, areas which had high transmission 20 and <10 years
499 ago, respectively, may highlight the impact of a reduced transmission in malaria immune responses. Still,
500 our data supports the notion that long-lived antibodies can be maintained even in the absence of ongoing
501 transmission. Of interest for countries aiming for elimination is evaluating the impact of a decrease in
502 transmission on the immunity or vulnerability of a population, especially in differing endemic settings
503 **(Fowkes et al., 2016; World Health Organization, 2017)**. Understanding the generation and maintenance
504 of effective immune responses during natural infection, particularly in the era of changing malaria
505 epidemiology, is crucial for the rational development and evaluation of future interventions and vaccines.
506 Immunological studies are needed to investigate this further.

507 Despite the mentioned limitations of the study, our results clearly show the potential use of multiplex antibody
508 responses and applications of machine learning approaches in assessing malaria transmission for countries
509 aiming for malaria elimination. In a sub-national elimination setting such as the Philippines, both recent and
510 historical *P. falciparum* and *P. vivax* exposure metrics were indicative of the absence of recent transmission
511 in Bataan and Occidental Mindoro, and were also able to identify current infections in Rizal, Palawan, thus
512 showing its ability in assessing the malaria situation in varying areas of endemicity. These serological
513 markers provide accurate estimates of recent and historical exposure to malaria and our study provides
514 baseline immunological data for monitoring risk populations. This serological surveillance approach can aid
515 in devising control measures by malaria elimination programs, as well as provide evidence of the
516 effectiveness of programs being implemented.

517 **Acknowledgements**

518 This study was supported by the Newton Fund, Philippine Council for Health Research and Development,
519 and UK Medical Research Council through funding received for ENSURE: Enhanced surveillance for control
520 and elimination of malaria in the Philippines (MR/N019199/1). We also express our gratitude to the ENSURE
521 team, specially Carol Joy Sarsadiaz, Hennessey Sabanal, Beulah Boncayao and Ellaine de la Fuente who
522 assisted in the conduct of serological assays for this project, as well as Dr. Mario Jiz, Dr. Catalino Demetria,
523 and Dr. Marilou Nicolas who provided technical assistance and access to their Luminex 200 instruments.
524 Also, we thank the local government and health staff of Palawan, Occidental Mindoro and Bataan for their
525 invaluable support to our research. This work is also supported by the Nagasaki University “Doctoral
526 Program for World-leading Innovative and Smart Education” for Global Health, “Global Health Elite
527 Programme for Building a Healthier World”.

528 **Author Contributions**

529 CJD, FEJE, JCRH, and MLMM conceived and designed this study. MLMM, KMF and CJD analyzed and
530 interpreted the data. MLMM wrote the first draft of the manuscript with support from KMF, CJD, JCRH, KY,
531 and FEJE. JSL, RAR, MLMM, and APNB supervised the data and sample collection, and the conduct of
532 assays. KKAT, JHA, CH, and CEC provided the recombinant antigens used for the multiplex bead-based
533 assay. MLMM and RAR performed the serological assays with support from TH and KKAT. All authors read
534 and approved the final manuscript.

535 **Competing interests**

536 The authors declare no competing interests.

537 **References**

- 538 Biggs J, Raman J, Cook J, Hlongwana K, Drakeley C, Morris N, et al. Serology reveals heterogeneity of
539 Plasmodium falciparum transmission in northeastern South Africa: Implications for malaria elimination. *Malar J*
540 2017;16. <https://doi.org/10.1186/s12936-017-1701-7>.
- 541 Burghaus PA, Holder AA. Expression of the 19-kilodalton carboxy-terminal fragment of the Plasmodium
542 falciparum merozoite surface protein-1 in Escherichia coli as a correctly folded protein. *Mol Biochem Parasitol*
543 1994;64:165–9. [https://doi.org/10.1016/0166-6851\(94\)90144-9](https://doi.org/10.1016/0166-6851(94)90144-9).
- 544 Chotirat S, Nekkab N, Kumpitak C, Hietanen J, White MT, Kiattitubtr K, et al. Application of 23 novel serological
545 markers for identifying recent exposure to Plasmodium vivax parasites in an endemic population of
546 western Thailand. *MedRxiv* 2021:2021.03.01.21252492.
- 547 Chuquiyauri R, Molina DM, Moss EL, Wang R, Gardner MJ, Brouwer KC, et al. Genome-scale protein microarray
548 comparison of human antibody responses in plasmodium vivax relapse and reinfection. *Am J Trop Med Hyg*
549 2015;93:801–9. <https://doi.org/10.4269/ajtmh.15-0232>.
- 550 Collins CR, Withers-Martinez C, Bentley GA, Batchelor AH, Thomas AW, Blackman MJ. Fine mapping of an
551 epitope recognized by an invasion-inhibitory monoclonal antibody on the malaria vaccine candidate apical
552 membrane antigen 1. *J Biol Chem* 2007;282:7431–41. <https://doi.org/10.1074/jbc.M610562200>.
- 553 Corran P, Coleman P, Riley E, Drakeley C. Serology: a robust indicator of malaria transmission intensity? *Trends*
554 *Parasitol* 2007;23:575–82. <https://doi.org/10.1016/j.pt.2007.08.023>.
- 555 Coutts SP, King JD, Pa’au M, Fuimaono S, Roth J, King MR, et al. Prevalence and risk factors associated with
556 lymphatic filariasis in American Samoa after mass drug administration. *Trop Med Health* 2017;45:1–10.
557 <https://doi.org/10.1186/s41182-017-0063-8>.
- 558 Crompton PD, Kayala MA, Traore B, Kayentao K, Ongoiba A, Weiss GE, et al. A prospective analysis of the Ab
559 response to Plasmodium falciparum before and after a malaria season by protein microarray. *Proc Natl Acad*
560 *Sci U S A* 2010;107:6958–63. <https://doi.org/10.1073/pnas.1001323107>.
- 561 Drakeley CJ, Corran PH, Coleman PG, Tongren JE, McDonald SLR, Carneiro I, et al. Estimating medium- and
562 long-term trends in malaria transmission by using serological markers of malaria exposure. *Proc Natl Acad Sci*
563 2005;102:5108–13. <https://doi.org/10.1073/pnas.0408725102>.
- 564 Folegatti PM, Siqueira AM, Monteiro WM, Lacerda MVG, Drakeley CJ, Braga ÉM. A systematic review on
565 malaria sero-epidemiology studies in the Brazilian Amazon: insights into immunological markers for exposure
566 and protection. *Malar J* 2017;16:107. <https://doi.org/10.1186/s12936-017-1762-7>.
- 567 Fornace KM, Brock PM, Abidin TR, Grignard L, Herman LS, Chua TH, et al. Environmental risk factors and
568 exposure to the zoonotic malaria parasite Plasmodium knowlesi across northern Sabah, Malaysia: a population-
569 based cross-sectional survey. *Lancet Planet Heal* 2019;3:e179–86. [https://doi.org/10.1016/S2542-5196\(19\)30045-2](https://doi.org/10.1016/S2542-5196(19)30045-2).
- 571 Fornace KM, Herman LS, Abidin TR, Chua TH, Daim S, Lorenzo PJ, et al. Exposure and infection to Plasmodium
572 knowlesi in case study communities in Northern Sabah, Malaysia and Palawan, The Philippines. *PLoS Negl Trop*
573 *Dis* 2018;12:e0006432. <https://doi.org/10.1371/journal.pntd.0006432>.
- 574 Fouda GG, Leke RFG, Long C, Druilhe P, Zhou A, Taylor DW, et al. Multiplex assay for simultaneous
575 measurement of antibodies to multiple Plasmodium falciparum antigens. *Clin Vaccine Immunol* 2006;13:1307–
576 13. <https://doi.org/10.1128/CVI.00183-06>.
- 577 Fowkes FJI, Boeuf P, Beeson JG. Immunity to malaria in an era of declining malaria transmission. *Parasitology*
578 2016;143:139–53. <https://doi.org/10.1017/S0031182015001249>.
- 579 Fowkes FJI, Richards JS, Simpson JA, Beeson JG. The relationship between anti-merozoite antibodies and
580 incidence of Plasmodium falciparum malaria: A systematic review and meta-analysis. *PLoS Med* 2010;7.
581 <https://doi.org/10.1371/journal.pmed.1000218>.
- 582 França CT, He WQ, Gruszczyk J, Lim NTY, Lin E, Kiniboro B, et al. Plasmodium vivax Reticulocyte Binding
583 Proteins Are Key Targets of Naturally Acquired Immunity in Young Papua New Guinean Children. *PLoS Negl*
584 *Trop Dis* 2016a;10:1–17. <https://doi.org/10.1371/journal.pntd.0005014>.

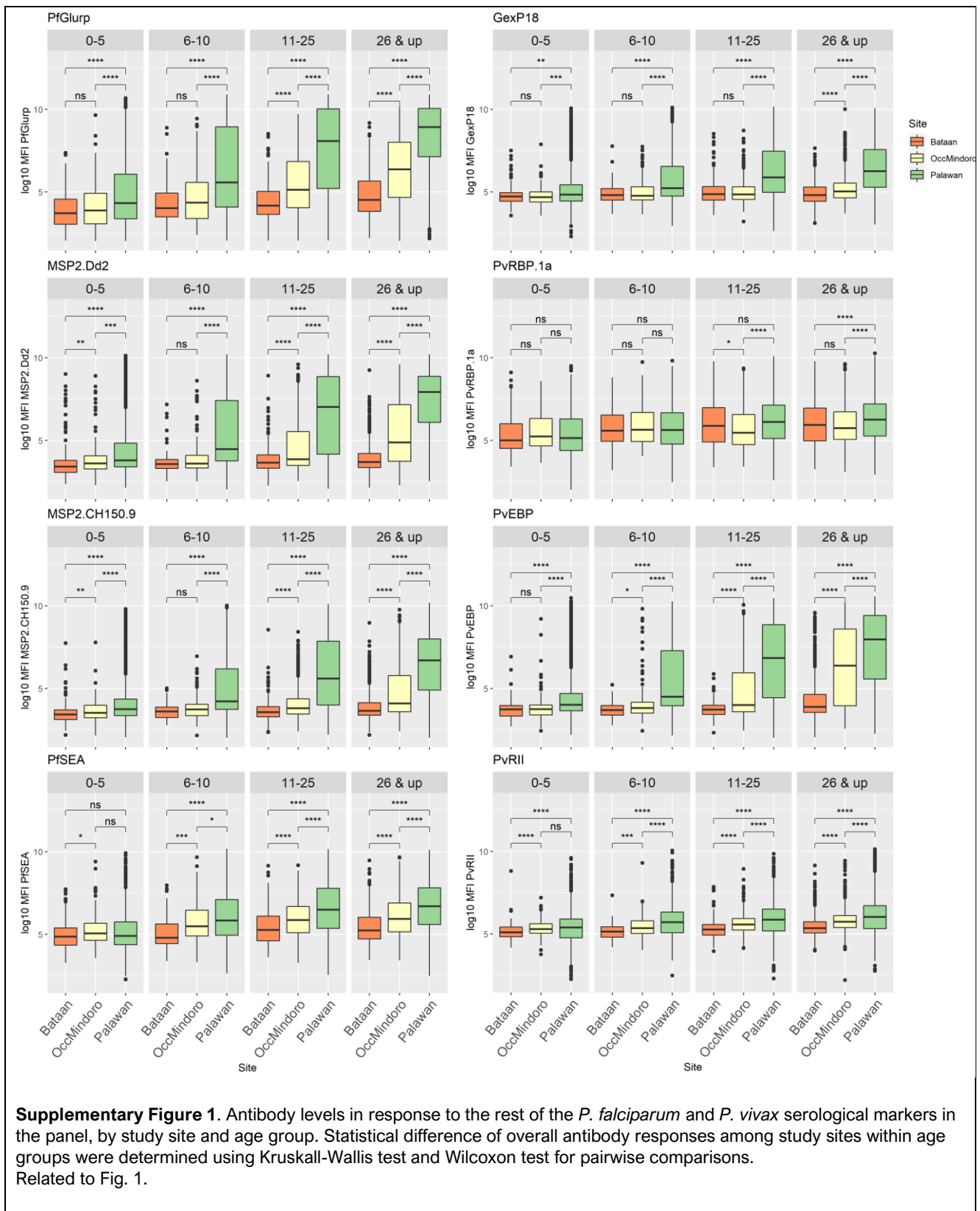
- 585 França CT, Hostetler JB, Sharma S, White MT, Lin E, Kiniboro B, et al. An Antibody Screen of a Plasmodium
586 vivax Antigen Library Identifies Novel Merozoite Proteins Associated with Clinical Protection. *PLoS Negl Trop*
587 *Dis* 2016b;10:1–15. <https://doi.org/10.1371/journal.pntd.0004639>.
- 588 Gnidehou S, Mitran CJ, Arango E, Banman S, Mena A, Medawar E, et al. Cross-species immune recognition
589 between plasmodium vivax duffy binding protein antibodies and the plasmodium falciparum surface antigen
590 VAR2CSA. *J Infect Dis* 2019;219:110–20. <https://doi.org/10.1093/infdis/jiy467>.
- 591 Helb DA, Tetteh KKA, Felgner PL, Skinner J, Hubbard A, Arinaitwe E, et al. Novel serologic biomarkers provide
592 accurate estimates of recent *Plasmodium falciparum* exposure for individuals and communities. *Proc Natl Acad*
593 *Sci* 2015;112:E4438–47. <https://doi.org/10.1073/pnas.1501705112>.
- 594 Hester J, Chan ER, Menard D, Mercereau-Puijalon O, Barnwell J, Zimmerman PA, et al. De Novo Assembly of a
595 Field Isolate Genome Reveals Novel Plasmodium vivax Erythrocyte Invasion Genes. *PLoS Negl Trop Dis* 2013;7.
596 <https://doi.org/10.1371/journal.pntd.0002569>.
- 597 van den Hoogen LL, Bareng P, Alves J, Reyes R, Macalinao M, Rodrigues JM, et al. Comparison of Commercial
598 ELISA Kits to Confirm the Absence of Transmission in Malaria Elimination Settings. *Front Public Heal* 2020a;8:1–
599 12. <https://doi.org/10.3389/fpubh.2020.00480>.
- 600 van den Hoogen LL, Griffin JT, Cook J, Sepúlveda N, Corran P, Conway DJ, et al. Serology describes a profile
601 of declining malaria transmission in Farafenni, The Gambia. *Malar J* 2015;14:416.
602 <https://doi.org/10.1186/s12936-015-0939-1>.
- 603 van den Hoogen LL, Prémumé J, Romilus I, Mondélus G, Elismé T, Sepúlveda N, et al. Quality control of
604 multiplex antibody detection in samples from large-scale surveys: the example of malaria in Haiti. *Sci Rep*
605 2020b;10:1–10. <https://doi.org/10.1038/s41598-020-57876-0>.
- 606 van den Hoogen LL, Stresman G, Prémumé J, Romilus I, Mondélus G, Elismé T, et al. Selection of Antibody
607 Responses Associated With Plasmodium falciparum Infections in the Context of Malaria Elimination. *Front*
608 *Immunol* 2020c;11:1–12. <https://doi.org/10.3389/fimmu.2020.00928>.
- 609 van den Hoogen LL, Walk J, Oulton T, Reuling IJ, Reiling L, Beeson JG, et al. Antibody Responses to Antigenic
610 Targets of Recent Exposure Are Associated With Low-Density Parasitemia in Controlled Human Plasmodium
611 falciparum Infections. *Front Microbiol* 2019;9:1–11. <https://doi.org/10.3389/fmicb.2018.03300>.
- 612 Hubbard A, Munoz ID, Decker A, Holcomb JB, Schreiber MA, Bulger EM, et al. Time-dependent prediction and
613 evaluation of variable importance using superlearning in high-dimensional clinical data. *J Trauma Acute Care*
614 *Surg* 2013;75:1–12. <https://doi.org/10.1097/TA.0b013e3182914553>.
- 615 Idris ZM, Chan CW, Mohammed M, Kalkoa M, Taleo G, Junker K, et al. Serological measures to assess the
616 efficacy of malaria control programme on Ambae Island, Vanuatu. *Parasites and Vectors* 2017;10.
617 <https://doi.org/10.1186/s13071-017-2139-z>.
- 618 Kerkhof K, Sluydts V, Willen L, Kim S, Canier L, Heng S, et al. Serological markers to measure recent changes
619 in malaria at population level in Cambodia. *Malar J* 2016;15:1–18. <https://doi.org/10.1186/s12936-016-1576-z>.
- 620 King CL, Davies DH, Felgner P, Baum E, Jain A, Randall A, et al. Biosignatures of Exposure/Transmission and
621 Immunity. *Am J Trop Med Hyg* 2015;93:16–27. <https://doi.org/10.4269/ajtmh.15-0037>.
- 622 Koffi D, Touré AO, Varela ML, Vigan-Womas I, Béourou S, Brou S, et al. Analysis of antibody profiles in
623 symptomatic malaria in three sentinel sites of Ivory Coast by using multiplex, fluorescent, magnetic, bead-based
624 serological assay (MAGPIX™). *Malar J* 2015;14. <https://doi.org/10.1186/s12936-015-1043-2>.
- 625 Longley RJ, White MT, Takashima E, Brewster J, Morita M, Harbers M, et al. Development and validation of
626 serological markers for detecting recent Plasmodium vivax infection. *Nat Med* 2020;26:741–9.
627 <https://doi.org/10.1038/s41591-020-0841-4>.
- 628 malERA Refresh Consultative Panel. malERA: An updated research agenda for characterising the reservoir and
629 measuring transmission in malaria elimination and eradication. *PLOS Med* 2017;14:e1002452.
630 <https://doi.org/10.1371/journal.pmed.1002452>.
- 631 Menard D, Chan ER, Benedet C, Ratsimbaoa A, Kim S, Chim P, et al. Whole Genome Sequencing of Field
632 Isolates Reveals a Common Duplication of the Duffy Binding Protein Gene in Malagasy Plasmodium vivax
633 Strains. *PLoS Negl Trop Dis* 2013;7. <https://doi.org/10.1371/journal.pntd.0002489>.
- 634 Mitran CJ, Yanow SK. The Case for Exploiting Cross-Species Epitopes in Malaria Vaccine Design. *Front*
635 *Immunol* 2020;11:1–14. <https://doi.org/10.3389/fimmu.2020.00335>.
- 636 Muh F, Kim N, Nyunt MH, Firdaus ER, Han JH, Hoque MR, et al. Cross-species reactivity of antibodies against

- 637 plasmodium vivax blood-stage antigens to plasmodium knowlesi. *PLoS Negl Trop Dis* 2020;14:1–21.
638 <https://doi.org/10.1371/journal.pntd.0008323>.
- 639 Niass O, Saint-Pierre P, Niang M, Diop F, Diouf B, Faye MM, et al. Modelling dynamic change of malaria
640 transmission in holoendemic setting (Dielmo, Senegal) using longitudinal measures of antibody prevalence to
641 Plasmodium falciparum crude schizonts extract. *Malar J* 2017;16:1–12. [https://doi.org/10.1186/s12936-017-](https://doi.org/10.1186/s12936-017-2052-0)
642 2052-0.
- 643 Ntumngia FB, Schloegel J, Barnes SJ, Mchenry AM, Singh S, King CL, et al. Conserved and variant epitopes of
644 Plasmodium vivax duffy binding protein as targets of inhibitory monoclonal antibodies. *Infect Immun*
645 2012;80:1203–8. <https://doi.org/10.1128/IAI.05924-11>.
- 646 Ondigo BN, Park GS, Gose SO, Ho BM, Ochola LA, Ayodo GO, et al. Standardization and validation of a
647 cytometric bead assay to assess antibodies to multiple Plasmodium falciparum recombinant antigens. *Malar J*
648 2012;11:1–17. <https://doi.org/10.1186/1475-2875-11-427>.
- 649 Perraut R, Richard V, Varela ML, Trape JF, Guillotte M, Tall A, et al. Comparative analysis of IgG responses to
650 Plasmodium falciparum MSP1p19 and PF13-DBL1 α 1 using ELISA and a magnetic bead-based duplex assay
651 (MAGPIX®-Luminex) in a Senegalese meso-endemic community. *Malar J* 2014;13.
652 <https://doi.org/10.1186/1475-2875-13-410>.
- 653 Polley SD, Conway DJ, Cavanagh DR, McBride JS, Lowe BS, Williams TN, et al. High levels of serum antibodies
654 to merozoite surface protein 2 of Plasmodium falciparum are associated with reduced risk of clinical malaria in
655 coastal Kenya. *Vaccine* 2006;24:4233–46. <https://doi.org/10.1016/j.vaccine.2005.06.030>.
- 656 Pothin E, Ferguson NM, Drakeley CJ, Ghani AC. Estimating malaria transmission intensity from Plasmodium
657 falciparum serological data using antibody density models. *Malar J* 2016;15:79. [https://doi.org/10.1186/s12936-](https://doi.org/10.1186/s12936-016-1121-0)
658 016-1121-0.
- 659 Proietti C, Krause L, Trieu A, Dodoo D, Gyan B, Koram KA, et al. Immune signature against Plasmodium
660 falciparum antigens predicts clinical immunity in distinct malaria endemic communities. *Mol Cell Proteomics*
661 2019:mcp.RA118.001256. <https://doi.org/10.1074/mcp.RA118.001256>.
- 662 Raj DK, Nixon CP, Nixon CE, Dvorin JD, DiPetrillo CG, Pond-Tor S, et al. Antibodies to PfSEA-1 block parasite
663 egress from RBCs and protect against malaria infection. *Science (80-)* 2014;344:871–7.
664 <https://doi.org/10.1126/science.1254417>.
- 665 Reyes RA, Fornace KM, Macalinao MLM, Boncayao BL, de la Fuente ES, Sabanal HM, et al. Enhanced health
666 facility surveys to support malaria control and elimination across different transmission settings in the
667 Philippines. *Am J Trop Med Hyg* 2021;104:968–78. <https://doi.org/10.4269/ajtmh.20-0814>.
- 668 Rogier E, Nace D, Dimbu PR, Wakeman B, Pohl J, Beeson JG, et al. Framework for Characterizing Longitudinal
669 Antibody Response in Children After Plasmodium falciparum Infection. *Front Immunol* 2021;12:1–11.
670 <https://doi.org/10.3389/fimmu.2021.617951>.
- 671 Rosado J, Pelleau S, Cockram C, Merklings SH, Nekkab N, Demeret C, et al. Multiplex assays for the
672 identification of serological signatures of SARS-CoV-2 infection: an antibody-based diagnostic and machine
673 learning study. *The Lancet Microbe* 2020;5247:1–10. [https://doi.org/10.1016/s2666-5247\(20\)30197-x](https://doi.org/10.1016/s2666-5247(20)30197-x).
- 674 Rosas-Aguirre A, Speybroeck N, Llanos-Cuentas A, Rosanas-Urgell A, Carrasco-Escobar G, Rodriguez H, et al.
675 Hotspots of malaria transmission in the Peruvian amazon: Rapid assessment through a parasitological and
676 serological survey. *PLoS One* 2015;10. <https://doi.org/10.1371/journal.pone.0137458>.
- 677 Sepúlveda N, Stresman G, White MT, Drakeley CJ. Current mathematical models for analyzing anti-malarial
678 antibody data with an eye to malaria elimination and eradication. *J Immunol Res* 2015;2015.
679 <https://doi.org/10.1155/2015/738030>.
- 680 Spielmann T, Ferguson DJP, Beck H-P. etramps , a New Plasmodium falciparum Gene Family Coding for
681 Developmentally Regulated and Highly Charged Membrane Proteins Located at the Parasite–Host Cell
682 Interface. *Mol Biol Cell* 2003;14:1529–44. <https://doi.org/10.1091/mbc.e02-04-0240>.
- 683 Ssewanyana I, Arinaitwe E, Nankabirwa JI, Yeka A, Sullivan R, Kamya MR, et al. Avidity of anti - malarial
684 antibodies inversely related to transmission intensity at three sites in Uganda. *Malar J* 2017:1–8.
685 <https://doi.org/10.1186/s12936-017-1721-3>.
- 686 Stanisci DI, Fowkes FJI, Koinari M, Javati S, Lin E, Kiniboro B, et al. Acquisition of antibodies against
687 Plasmodium falciparum merozoites and malaria immunity in young children and the influence of age, force of
688 infection, and magnitude of response. *Infect Immun* 2015;83. <https://doi.org/10.1128/IAI.02398-14>.
- 689 Taylor RR, Smith DB, Robinson VJ, McBride JS, Riley EM. Human antibody response to Plasmodium falciparum

- 690 merozoite surface protein 2 is serogroup specific and predominantly of the immunoglobulin G3 subclass. *Infect*
691 *Immun* 1995;63:4382–8. <https://doi.org/10.1128/iai.63.11.4382-4388.1995>.
- 692 Theisen M, Vuust J, Gottschau A, Jepsen S, Hogh B. Antigenicity and immunogenicity of recombinant
693 glutamate-rich protein of *Plasmodium falciparum* expressed in *Escherichia coli*. *Clin Diagn Lab Immunol*
694 1995;2:30–4. <https://doi.org/10.1128/cdli.2.1.30-34.1995>.
- 695 World Health Organization. World Malaria Report 2019. vol. WHO/HTM/GM. Geneva, Switzerland: 2019.
- 696 World Health Organization. WHO malaria policy advisory committee meeting: meeting report, October 2017.
697 Geneva, Switzerland: 2017.
- 698 World Health Organization. Progress towards subnational elimination in the Philippines. Geneva PP - Geneva:
699 World Health Organization; 2014.
- 700 World Health Organization, Global Malaria Programme. A Framework for Malaria Elimination. 2017.
701 [https://doi.org/Licence: CC BY-NC-SA 3.0 IGO](https://doi.org/Licence:CC-BY-NC-SA-3.0-IGO).
- 702 Wu L, Hall T, Ssewanyana I, Oulton T, Patterson C, Vasileva H, et al. Optimisation and standardisation of a
703 multiplex immunoassay of diverse *Plasmodium falciparum* antigens to assess changes in malaria transmission
704 using sero-epidemiology. *Wellcome Open Res* 2019;4:26. <https://doi.org/10.12688/wellcomeopenres.14950.1>.
- 705 Wu L, Mwesigwa J, Affara M, Bah M, Correa S, Hall T, et al. Sero-epidemiological evaluation of malaria
706 transmission in The Gambia before and after mass drug administration. *BMC Med* 2020a;18:1–14.
707 <https://doi.org/10.1186/s12916-020-01785-6>.
- 708 Wu L, Mwesigwa J, Affara M, Bah M, Correa S, Hall T, et al. Antibody responses to a suite of novel serological
709 markers for malaria surveillance demonstrate strong correlation with clinical and parasitological infection across
710 seasons and transmission settings in The Gambia. *BMC Med* 2020b:2020.07.10.20067488.
711 <https://doi.org/10.1101/2020.07.10.20067488>.

712

713

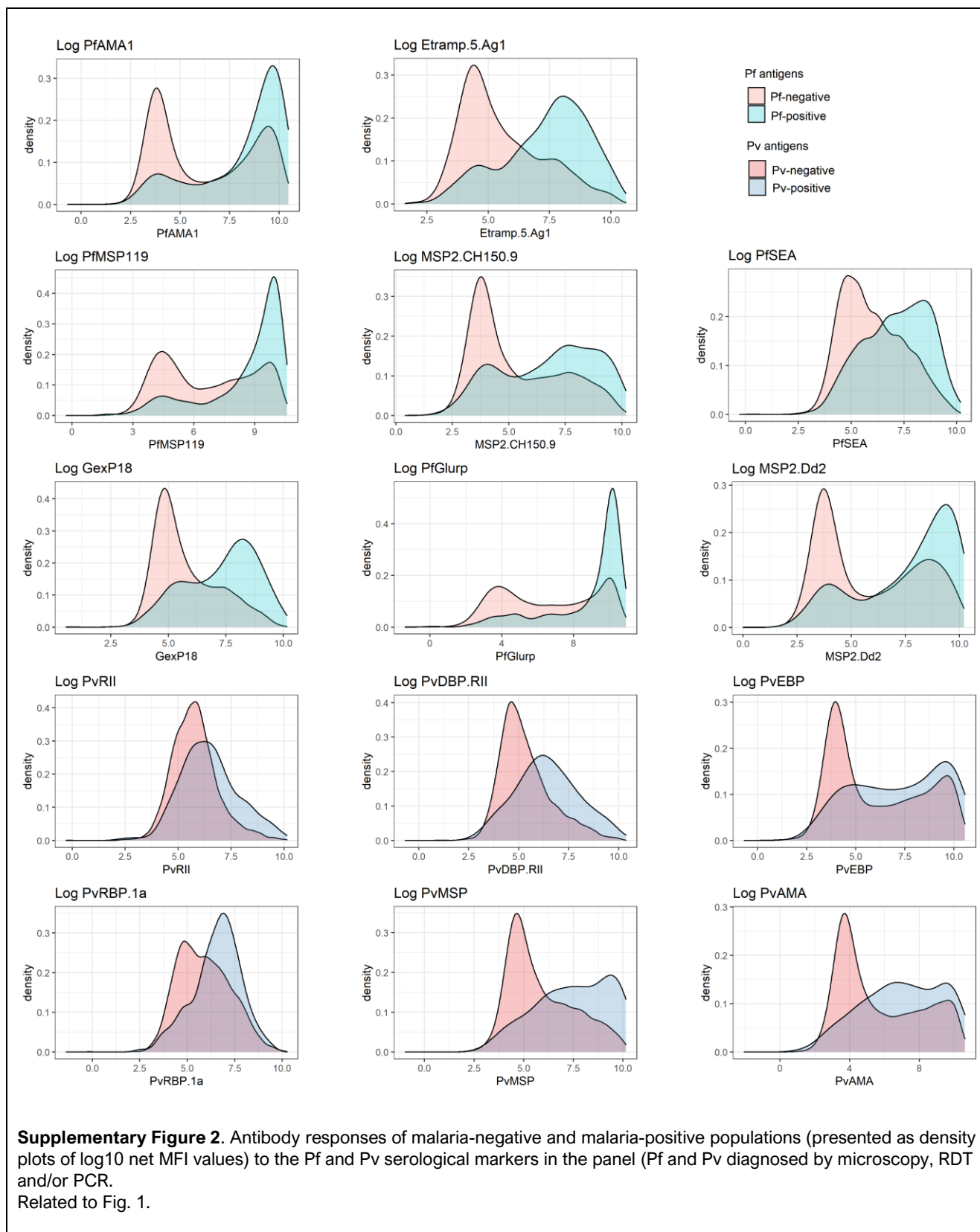


Supplementary Figure 1. Antibody levels in response to the rest of the *P. falciparum* and *P. vivax* serological markers in the panel, by study site and age group. Statistical difference of overall antibody responses among study sites within age groups were determined using Kruskal-Wallis test and Wilcoxon test for pairwise comparisons. Related to Fig. 1.

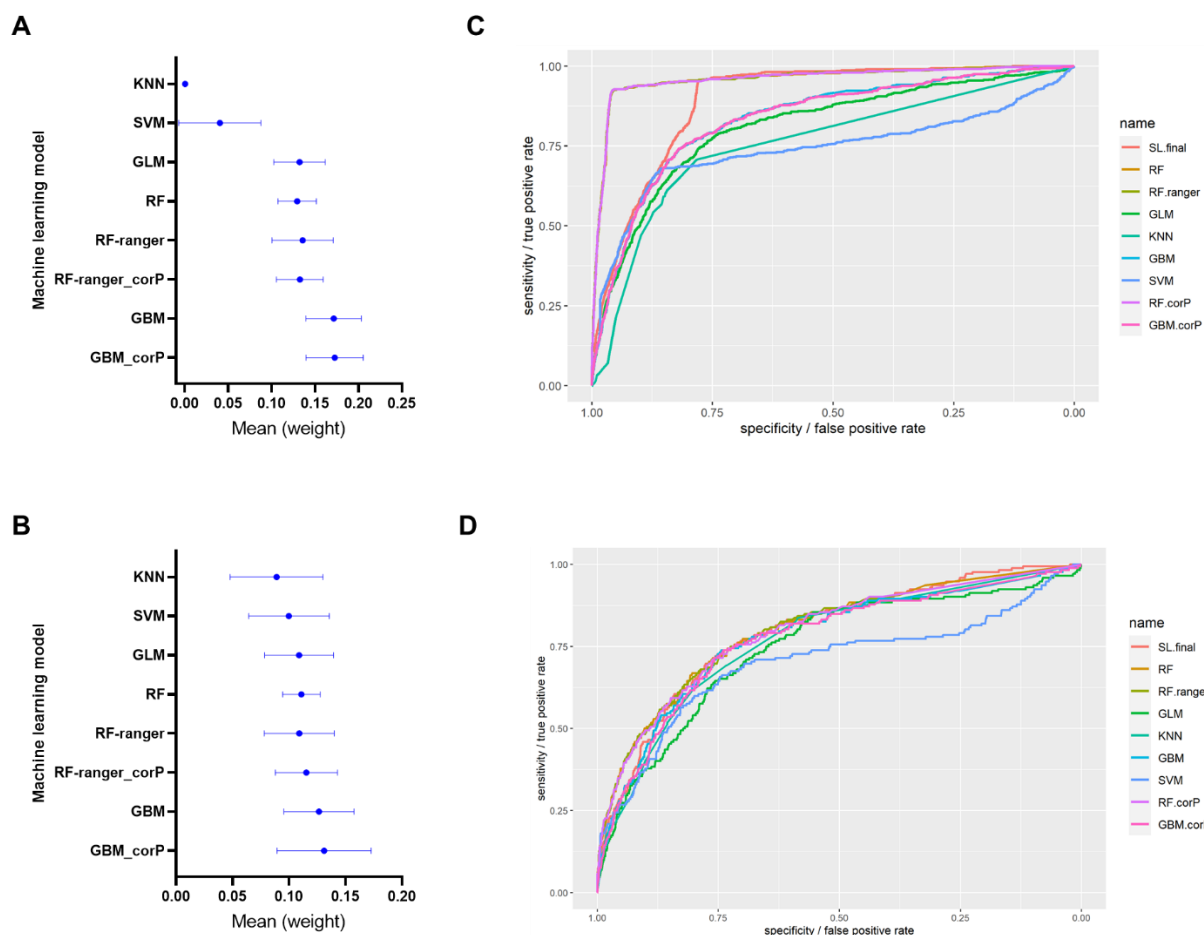
714

715

716



717



Supplementary Figure 3. Performances of the individual base learners in the Super Learner ensemble.

A-B) Plots of the assigned weights to each learner included in the Super Learner models for predicting *P. falciparum* (A) and *P. vivax* recent exposure (B), obtained after 20-fold nested cross-validation of the Pf SL-covar8 and Pv SL-covar6 models.

C-D) Receiver operating characteristic (ROC) curves for detecting current Pf (C) and Pv (D) infections in the test dataset (n=9132) using the 8 Pf and 6 Pv antigens as covariates, respectively. (SL.final: final Super Learner model, RF: random Forest, RF.ranger: RF from ranger package, kNN: k-Nearest Neighbor, GBM: generalized boosted models (implementation for BRT: boosted regression trees), SVM:Support Vector Machine, and GLM: Generalized linear models; variation of algorithms with “corP” denotes a feature selection that screens for univariate correlation)

Supplementary Table 1. Seropositivity rates based on Pf-specific antigens and SuperLearner predictions for recent Pf exposure

Model	Seropositivity cutoff value for antigens	AUC – validation data	AUC – study data	Positive in Pf+ samples (n=625)	Positive in Palawan, n=6572 (%)	Positive in Occidental Mindoro, n=1683 (%)	Positive in Bataan, n=877 (%)
PfAMA1	FMM	129.552007	0.9075 (0.8866-0.9284)	0.6921 (0.6771-0.7072)	509 (85.5%)	3842 (58.5%)	91 (10.4%)
	Negpop	146.705091	0.9115 (0.892-0.9311)	0.6948 (0.6795-0.71)	507 (85.2%)	3792 (57.7%)	82 (9.4%)
PfMSP1 ₁₉	FMM	315.978321	0.9321 (0.9182-0.9459)	0.6849 (0.6696-0.7002)	503 (84.5%)	3872 (58.9%)	85 (9.7%)
	Negpop	294.522036	0.9301 (0.9152-0.9449)	0.6821 (0.667-0.6973)	508 (85.4%)	3940 (60.0%)	89 (10.1%)
Etramp5.Ag1	FMM	343.006451	0.9075 (0.8918-0.9232)	0.7556 (0.7389-0.7722)	477 (80.2%)	2659 (40.5%)	60 (6.8%)
	Negpop	254.493948	0.9111 (0.8941-0.9281)	0.7397 (0.7235-0.7559)	489 (82.2%)	2963 (45.1%)	87 (9.9%)
GEXP18	FMM	402.149776	0.8848 (0.8663-0.9033)	0.7456 (0.7278-0.7633)	452 (76.0%)	2524 (38.4%)	65 (7.4%)
	Negpop	267.001733	0.9037 (0.8849-0.9225)	0.7317 (0.7154-0.748)	487 (81.8%)	3067 (46.7%)	126 (14.4%)
PfGLURP R2	FMM	346.692889	0.9206 (0.901-0.9401)	0.6849 (0.6701-0.6997)	516 (86.7%)	3817 (58.1%)	147 (16.8%)
	Negpop	361.031502	0.9254 (0.9074-0.9435)	0.6855 (0.6706-0.7004)	512 (86.1%)	3810 (58.0%)	143 (16.3%)
MSP2 CH150/9	FMM	137.354929	0.8558 (0.8325-0.879)	0.6849 (0.6665-0.7034)	437 (73.4%)	3093 (47.1%)	76 (8.7%)
	Negpop	141.708302	0.8541 (0.8307-0.8774)	0.4971 (0.4921-0.5022)	437 (73.4%)	3074 (46.8%)	75 (8.6%)
MSP2 Dd2	FMM	121.316261	0.9177 (0.9027-0.9326)	0.6762 (0.6598-0.6926)	484 (81.3%)	3673 (55.9%)	126 (14.4%)
	Negpop	110.971531	0.9202 (0.9054-0.935)	0.6798 (0.6632-0.6965)	482 (81.0%)	3607 (54.9%)	105 (12.0%)
PfSEA	FMM	733.501223	0.8207 (0.7975-0.844)	0.6714 (0.6515-0.6912)	384 (64.5%)	2387 (36.3%)	131 (14.9%)
	Negpop	867.158828	0.8121 (0.7918-0.8324)	0.6614 (0.6411-0.6816)	357 (60.0%)	2203 (33.5%)	112 (12.8%)
Random Forest: 4 covariates (RF.covar4)	(Etramp5.Ag1, GEXP18, PfGLURP R2, PfMSP1 ₁₉)	0.9983 (0.996-1)	0.9591 (0.9497-0.9684)	552 (92.8%)	1081 (16.4%)	5 (0.3%)	1 (0.1%)
Random Forest: 8 covariates (RF.covar8)	All 8 Pf-specific antigens	0.9898 (0.998-1)	0.9682 (0.9605-0.9759)	555 (93.3%)	1065 (16.2%)	3 (0.2%)	0 (0.0%)
SL: 3 covariates (SL:3-covar)	(Etramp5.Ag1, GEXP18, PfGLURP R2)	0.918 (0.9067-0.9293)	0.879 (0.8658-0.8921)	265 (44.5%)	809 (12.3%)	0 (0.0%)	0 (0.0%)
SL: 4 covariates (SL:4-covar)	(Etramp5.Ag1, GEXP18, PfGLURP R2, PfMSP1 ₁₉)	0.9338 (0.9214-0.9462)	0.8967 (0.8867-0.9067)	297 (49.9%)	687 (10.5%)	0 (0.0%)	0 (0.0%)
SL: 8 covariates (SL:8-covar)	All 8 Pf-specific antigens	0.955 (0.9486-0.9614)	0.914 (0.9055-0.9226)	317 (53.3%)	828 (12.6%)	0 (0.0%)	0 (0.0%)
SL: 9 covariates (SL:9-covar)	All 8 Pf-specific antigens and age	0.9898 (0.9874-0.9921)	0.9197 (0.9093-0.9302)	423 (71.1%)	1245 (18.9%)	4 (0.2%)	0 (0.0%)

*Abbreviations used: Pf: *P. falciparum*; FMM: Finite mixture model; Negpop: Negative population model; SL: Super Learner prediction model using different sets of covariates (including the 8 Pf antigens) for predicting recent and historical malaria exposure.

Supplementary Table 2. Seropositivity rates based on 6 Pv-specific antigens and SuperLearner predictions for recent Pv exposure

Model		Seropositivity cutoff value for antigens	AUC – validation data	AUC – study data	Positive in Pv+ samples (n=172)	Positive in Palawan, n=6572 (%)	Positive in Occidental Mindoro, n=1683 (%)	Positive in Bataan, n=877 (%)
PvAMA1	FMM	149.776739	0.9185 (0.8934 - 0.9436)	0.6744 (0.6424 - 0.7064)	130 (75.6%)	2991 (45.5%)	650 (38.6%)	84 (9.6%)
	Negpop	172.486298	0.9164 (0.8895 - 0.9434)	0.6720 (0.6391 - 0.7049)	127 (73.8%)	3035 (46.2%)	626 (37.2%)	77 (8.8%)
PvMSP1 ₁₉	FMM	395.678911	0.9429 (0.9229 - 0.9629)	0.7308 (0.6997 - 0.7618)	134 (77.9%)	2588 (39.4%)	430 (25.5%)	63 (7.2%)
	Negpop	666.248684	0.9234 (0.8935 - 0.9533)	0.7049 (0.6692 - 0.7406)	114 (66.3%)	2135 (32.5%)	295 (17.5%)	38 (4.3%)
PvDBP.RII	FMM	403.658933	0.8036 (0.7546 - 0.8527)	0.7065 (0.6697 - 0.7434)	105 (61.0%)	1699 (25.9%)	165 (9.8%)	50 (5.7%)
	Negpop	285.09444	0.8143 (0.7668 - 0.8618)	0.7037 (0.6681 - 0.7392)	115 (66.9%)	2087 (31.8%)	221 (13.1%)	72 (8.2%)
PvRBP.1a	FMM	777.354467	0.7367 (0.6865 - 0.7869)	0.6248 (0.5871 - 0.6625)	92 (53.5%)	1979 (30.1%)	416 (24.7%)	242 (27.6%)
	Negpop	2986.35245	0.5343 (0.5006 - 0.5679)	0.5127 (0.4901 - 0.5352)	17 (9.9%)	507 (7.7%)	104 (6.2%)	61 (7.0%)
PvRII	FMM	843.409764	0.7706 (0.7195 - 0.8218)	0.6302 (0.5935 - 0.6670)	67 (39.0%)	1079 (16.4%)	104 (6.2%)	38 (4.3%)
	Negpop	377.466964	0.8007 (0.7530 - 0.8484)	0.6322 (0.5955 - 0.6688)	107 (62.2%)	2717 (41.3%)	489 (29.1%)	102 (11.6%)
PvEBP	FMM	147.668259	0.7735 (0.7247 - 0.8224)	0.6471 (0.6144 - 0.6799)	128 (74.4%)	3328 (50.6%)	719 (42.7%)	106 (12.1%)
	Negpop	661.785062	0.7133 (0.6616 - 0.7649)	0.6184 (0.5809 - 0.6559)	101 (58.7%)	2608 (39.7%)	566 (33.6%)	63 (7.2%)
SL: 6 Pv antigens	All Pv-specific antigens as covariates		0.8857 (0.8429-0.9284)	0.6332 (0.5979-0.6686)	57 (33.1%)	603 (9.2%)	35 (2.1%)	2 (0.2%)
RF: 6 Pv antigens			1	0.6918 (0.6542-0.7293)	81 (47.1%)	802 (12.2%)	57 (3.4%)	5 (0.6%)
GBM: 6 Pv antigens			0.9043 (0.8647-0.9439)	0.6462 (0.6095-0.6828)	67 (39.0%)	851 (12.9%)	80 (4.8%)	7 (0.8%)

*Abbreviations used: Pv: *P. vivax*; FMM: Finite mixture model; Negpop: Negative population model; SL: Superlearner prediction model using different sets of covariates (including the 8 Pf antigens) for predicting recent and historical malaria exposure.

722 **Tables and figures**

723 **Tables**

724 **Table 1.** List of antigens in the multiplex bead-based assay panel

725 **Table 2.** Training and validation data used in the classification models

726 **Table 3.** Characteristics of study population by site

727 **Table 4.** Seroconversion and seroreversion rates from reverse catalytic models in each study site

728 **Supplementary Table 1.** Seropositivity rates based on Pf-specific antigens and SuperLearner predictions
729 for recent Pf exposure

730 **Supplementary Table 2.** Seropositivity rates based on 6 Pv-specific antigens and SuperLearner
731 predictions for recent Pv exposure

732 **Figures**

733 **Figure 1.** Map showing the study sites, with red areas as the focused municipalities within the provinces
734 marked yellow.

735 **Figure 2. Antibody responses to serological markers of *P. falciparum* and *P. vivax* correlate with
736 malaria incidence**

737 **A.** Antibody levels (reported as log₁₀ MFI) in response to *P. falciparum* cumulative and recent exposure
738 markers PfAMA1, PfMSP1₁₉, and Etramp5.Ag1, and *P. vivax* serological markers PvAMA1, PvMSP1₁₉
739 and PvDBP.RII by study site and age group. Statistical difference of overall antibody responses
740 among study sites within age groups were determined using Kruskal-Wallis test and Wilcoxon test
741 for pairwise comparisons (*p < 0.05, **p < 0.01, ***p < 0.001, ****p < 0.0001).

742 **B.** Spearman's correlation coefficients for age, malaria diagnosis (Mal+: Plasmodium-positive, Pf+: *P.*
743 *falciparum*-positive, Pv+: *P. vivax*-positive), and antibody responses to the 14 antigens in the panel
744 for Palawan samples (n=6572).

745 **Figure 3. Serological markers exhibit species-specific association with current infection in varying
746 levels**

747 **A-B)** Comparison of antibody titers of Palawan samples (n=6572) for *Plasmodium*-positive (Pf: *P.*
748 *falciparum*-positive, Pf/Pv: Pf and Pv mixed infection, Pv: *P. vivax*-positive) and negative (neg)
749 samples by age group in each *P. falciparum*-specific (A) and *P. vivax*-specific antigen.

750 **Figure 4. Analysis of serological markers through machine learning methods improves
751 classifications for recent *P. falciparum* and *P. vivax* exposure or current infection**

752 **A-B.** Seropositivity rates of sample population by site and age group based on cutoff values from finite
753 mixture models (FMM) and negative population model (NegPop) for Pf and Pv antigens (detailed
754 in **Supplementary Tables 1 and 2**). Hollow dots represent the FMM and Negpop seropositivity
755 rates for the two reported recent exposure markers Etramp5.Ag1 and GEXP18 for Pf (A), and
756 PvMSP1₁₉ and PvDBP.RII for Pv (B) panel. Lines with error bars represent median with 95% CI.

757 **C-D.** Receiver operating characteristic (ROC) curves for the antibody responses to single antigens for
758 individual antigens, and for the SL models (shown in both as binary outcomes of seropositivity /
759 prediction values).

760 **E-F.** Variable importance of the 8 Pf-specific (E) and 6 Pv-specific (F) antigens based on the Random
761 Forest model.

762 **G.** Predicted rates of recent Pf exposure based on analysis of the continuous antibody responses of the
763 8-antigen panel using Super Learner. Each hollow dot represents differences in the number of
764 covariates used for the model (3, 4, 8, 9), as well as 2 showing rates from prediction values of the
765 Random Forests (RF) component model (RF.covar4 and RF.covar8 in solid dots).

766 **H.** Predicted rates of recent Pv exposure based on analysis of the continuous antibody responses of the
767 6-antigen panel using Super Learner. Dots represent the positivity rates from the prediction

768 values of the SL model, and the individual predictions from the 2 most weighted base learners in
769 the resulting model – RF and GBM. RF predictions (RF.covar6) are shown as solid dots.
770 (SL: Super Learner, RF: random Forest, covar#: number of covariates included in the model, FMM: finite
771 mixture models; *p < 0.05, **p < 0.01, ***p < 0.001, ****p < 0.0001 with significance assessed by one-way
772 ANOVA followed by Tukey’s multiple comparison)

773 **Figure 5. Seroconversion curves based on reverse catalytic models using AMA1 and MSP1₁₉**
774 **antibody responses provide accurate estimates of historical exposure.**

775 Age-specific seroprevalence was based on finite mixture models and Random Forest models (using both
776 antigens: RF 2-covar models) for each species. Solid lines represent the fit of the reversible catalytic
777 models, dashed lines represent 95% confidence intervals, and dots represent the observed proportions of
778 seropositives per age divided into 10% centiles. For models assuming a change point in transmission, only
779 the recent seroconversion rates and change point estimates (in years) are shown, while the historical
780 seroconversion rates and seroreversion rates are detailed in Table 4.

781 **Figure 6. Cumulative exposure markers confirm historical *P. falciparum* and *P. vivax* exposure, and**
782 **heterogeneity of transmission in the 3 sites**

- 783 **A.** Plot of Super Learner prediction values for Pf historical exposure by site and age, using the model
784 with 8 Pf-specific serological markers as covariates. Red dotted line represents positivity cutoff at 0.5.
785 **B.** Variable importance based on the Random Forest model of the 8 Pf-specific antigens and 6 Pv-
786 specific antigens in predicting historical exposure for each species.
787 **C.** Distribution of antibody responses to PfAMA1 by site and age of individuals (n=9132). Red dashed
788 line represents the seropositivity cutoff value from the FMM model.
789 **D-E.** Summary graphs per age category per site of SL-predicted Pf historical exposure (D) and PfAMA1,
790 PfMSP1 seropositivity rates graphed with estimated historical exposure rates using the Random
791 Forest model with PfAMA1, PfMSP1₁₉ as covariates (E).
792 **F.** Summary graph of PvAMA1, PvMSP1 seropositivity rates with estimated historical exposure rates
793 using the Random Forest model with PvAMA1, PvMSP1₁₉ as covariates seropositivity per age
794 category per site

795 **Supplementary Figure 1.** Antibody levels in response to the rest of the *P. falciparum* and *P. vivax*
796 serological markers in the panel, by study site and age group. Statistical difference of overall antibody
797 responses among study sites within age groups were determined using Kruskal-Wallis test and Wilcoxon
798 test for pairwise comparisons. Related to Fig. 1.

799 **Supplementary Figure 2.** Antibody responses of malaria-negative and malaria-positive populations
800 (presented as density plots of log₁₀ net MFI values) to the Pf and Pv serological markers in the panel (Pf
801 and Pv diagnosed by microscopy, RDT and/or PCR. Related to Fig. 1.

802 **Supplementary Figure 3. Performances of the individual base learners in the Super Learner**
803 **ensemble.**

- 804 **A-B)** Plots of the assigned weights to each learner included in the Super Learner models for predicting *P.*
805 *falciparum* (A) and *P. vivax* recent exposure (B), obtained after 20-fold nested cross-validation of the
806 Pf SL-covar8 and Pv SL-covar6 models.
807 **C-D)** Receiver operating characteristic (ROC) curves for detecting current Pf (C) and Pv (D) infections in
808 the test dataset (n=9132) using the 8 Pf and 6 Pv antigens as covariates, respectively. (SL.final: final
809 Super Learner model, RF: random Forest, RF.ranger: RF from ranger package, kNN: k-Nearest
810 Neighbor, GBM: generalized boosted models (implementation for BRT: boosted regression trees),
811 SVM: Support Vector Machine, and GLM: Generalized linear models; variation of algorithms with
812 “corP” denotes a feature selection that screens for univariate correlation)

813